The GGCMI phase II emulators: global gridded crop model responses to changes in CO$_2$, temperature, water, and nitrogen (version 1.0)

James Franke[1,2], Christoph Müller[3], Joshua Elliott[2,4], Alex C. Ruane[5], Jonas Jägermeyr[4,2,3,5], Abigail Snyder[6], Marie Dury[7], Pete Falloon[8], Christian Folberth[9], Louis François[7], Tobias Hank[10], R. Cesar Izaurralde[11,12], Ingrid Jacquemin[7], Curtis Jones[11], Michelle Li[2,13], Wenfeng Liu[14,15], Stefan Olin[16], Meridel Phillips[5,17], Thomas A. M. Pugh[18,19], Ashwan Reddy[11], Karina Williams[8], Ziwei Wang[1,2], Florian Zabel[10], and Elisabeth Moyer[1,2]

[1]Department of the Geophysical Sciences, University of Chicago, Chicago, IL, USA
[2]Center for Robust Decision-making on Climate and Energy Policy (RDCEP), University of Chicago, Chicago, IL, USA
[3]Potsdam Institute for Climate Impact Research, Member of the Leibniz Association, Potsdam, Germany
[4]Department of Computer Science, University of Chicago, Chicago, IL, USA
[5]NASA Goddard Institute for Space Studies, New York, NY, United States
[6]Joint Global Change Research Institute, Pacific Northwest National Laboratory, College Park, MD, USA
[7]Unité de Modélisation du Climat et des Cycles Biogéochimiques, UR SPHERES, Institut d'Astrophysique et de Géophysique, University of Liège, Belgium
[8]Met Office Hadley Centre, Exeter, United Kingdom
[9]Ecosystem Services and Management Program, International Institute for Applied Systems Analysis, Laxenburg, Austria
[10]Department of Geography, Ludwig-Maximilians-Universität, Munich, Germany
[11]Department of Geographical Sciences, University of Maryland, College Park, MD, USA
[12]Texas Agrilife Research and Extension, Texas A&M University, Temple, TX, USA
[13]Department of Statistics, University of Chicago, Chicago, IL, USA
[14]EAWAG, Swiss Federal Institute of Aquatic Science and Technology, Dübendorf, Switzerland
[15]Laboratoire des Sciences du Climat et de l'Environnement, LSCE/IPSL, CEA-CNRS-UVSQ, Université Paris-Saclay, F-91191 Gif-sur-Yvette, France.
[16]Department of Physical Geography and Ecosystem Science, Lund University, Lund, Sweden
[17]Earth Institute Center for Climate Systems Research, Columbia University, New York, NY, USA
[18]School of Geography, Earth and Environmental Sciences, University of Birmingham, Birmingham, UK.
[19]Birmingham Institute of Forest Research, University of Birmingham, Birmingham, UK.

Correspondence: James Franke (jfranke@uchicago.edu)

Abstract. Statistical emulation allows combining advantageous features of statistical and process-based crop models for understanding the effects of future climate changes on crop yields. We describe here the development of emulators for nine process-based crop models and five crops using output from the Global Gridded Model Intercomparison Project (GGCMI) Phase II. The GGCMI Phase II experiment is designed with the explicit goal of producing a structured training dataset for emulator development that samples across four dimensions relevant to crop yields: atmospheric carbon dioxide (CO$_2$) concentrations, temperature, water supply, and nitrogen inputs (CTWN). Simulations are run under two different adaptation assumptions: that growing seasons shorten in warmer climates, and that cultivar choice allows growing seasons to remain fixed. The dataset allows emulating the climatological mean yield response without relying on interannual variations; we show that these

are quantitatively different. Climatological mean yield responses can be readily captured with a simple polynomial in nearly

10 all locations, with errors significant only in some marginal lands where crops are not currently grown. In general, emulation errors are negligible relative to differences across crop models or even across climate model scenarios. We demonstrate that the resulting GGCMI emulators can reproduce yields under realistic future climate simulations, even though the GGCMI Phase II dataset is constructed with uniform CTWN offsets, suggesting that the effects of changes in temperature and precipitation distributions are small relative to those of changing means. The resulting emulators therefore capture relevant crop model re-

15 sponses in a lightweight, computationally tractable form, providing a tool that can facilitate model comparison, diagnosis of interacting factors affecting yields, and integrated assessment of climate impacts.

1 Introduction

Improving our understanding of the impacts of future climate change on crop yields is critical for global food security in the twenty-first century. Projections of future yields under climate change are generally made with one of two approaches: either

20 process-based models, which simulate the process of photosynthesis and the biology and phenology of individual crops, or statistical models, which use historical weather and yield data to capture relationships between observed crop yields and major drivers. Process-based crop models provide some advantages, including capturing the direct effects of CO_2 fertilization and allowing projections in areas where crops are not currently grown. However, they are computationally expensive, and can be difficult or impossible to directly integrate into integrated climate change impacts assessments. Statistical crop models can only

25 capture crop responses under the range of current conditions, but have several advantages: they implicitly include management and behavioral practices that are difficult to model explicitly, and they are typically simple analytical expressions that are easily implemented by downstream impact modelers. Both types of models are routinely used, and comparative studies have concluded that when done carefully, both approaches can provide similar yield estimates (e.g. Lobell and Burke, 2010; Moore et al., 2017; Roberts et al., 2017; Zhao et al., 2017; Liu et al., 2016a).

30 Statistical emulation allows combining some of the advantageous features of both statistical and process-based models. The approach involves constructing a "surrogate model" of numerical simulations by using their output as training data for a statistical representation (e.g. O'Hagan, 2006; Conti et al., 2009). Emulation is particularly useful in cases where simulations are complex and output data volumes are large, and has been used in a variety of fields, including hydrology (e.g. Razavi et al., 2012), engineering (e.g. Storlie et al., 2009), environmental sciences (e.g. Ratto et al., 2012), and climate (e.g. Castruccio

35 et al., 2014; Holden et al., 2014). For agricultural impacts studies, emulation of process-based models allows capturing key relationships between input variables in a lightweight, flexible form that is compatible with economic studies. The resultant statistical model can produce yield projections under arbitrary emissions scenarios and is an important diagnostic tool for model comparison and model evaluation.

Interest is rising in applying statistical emulation to crop models, and multiple studies have developed crop model emulators

40 in the past decade. Early studies proposing or describing potential crop yield emulators include Howden and Crimp (2005); Räisänen and Ruokolainen (2006); Lobell and Burke (2010), and Ferrise et al. (2011). Studies developing single-model emula-

tors include Holzkämper et al. (2012) for the CropSyst model, Ruane et al. (2013) for the CERES wheat model, and Oyebamiji et al. (2015) for the LPJmL model. More recently, emulators have begun to be used in the context of multi-model intercomparison, with multiple authors (Blanc and Sultan, 2015; Blanc, 2017; Ostberg et al., 2018; Mistry et al., 2017) using them to

45   analyze the five crop models of the Inter-Sectoral Impact Model Intercomparison Project (ISIMIP). ISIMIP offers a relatively large training set – control, historical, and several Representative Concentration Pathway (RCP) scenarios using output from up to five climate models (Warszawski et al., 2014; Frieler et al., 2017) – and choices of emulation strategy differ. Blanc and Sultan (2015) and Blanc (2017) use historical and RPC8.5 scenarios, combine multiple climate model projections for RCP8.5, and regress across soil regions. Ostberg et al. (2018) use global mean temperature change (and CO_2) as regressors, and then

50   pattern-scales to emulate local yields. Mistry et al. (2017) compare emulated and observed historical yields, using local weather data and a historical crop simulation. The constraints of the ISIMIP experiment mean that all these efforts do share important common features. All emulate annual crop yields along an entire scenario or scenarios, and all future climate scenarios are non-stationary, with important covariates (temperature and precipitation for example) evolving simultaneously.

An alternative approach to emulation involves construction of a "parameter sweep" training set, a collection of multiple

55   stationary scenarios that systematically cover a range of input parameter values. A parameter sweep offers several important advantages for emulation over an experiment in which climate evolves over time. First, it allows separating the effects of different variables that affect yields but that are highly correlated in realistic future scenarios like those used in ISIMIP (e.g. CO_2 and temperature). Second, it allows making a distinction between year-to-year yield variations and climatological changes, which may involve different responses to the particular climate regressors used (e.g. Ruane et al., 2016). For example, if year-

60   to-year yield variations are driven predominantly by variations in the distribution of temperatures throughout the growing period, and long-term climate changes are driven predominantly by additive mean shifts, then regressing on the mean growing period temperature will produce different yield responses at annual vs. climatological timescales.

Systematic parameter sweeps have begun to be used in crop model evaluation and emulation, with early efforts in 2014 and 2015 (Ruane et al., 2014; Makowski et al., 2015; Pirttioja et al., 2015), and several recent studies in 2018 and 2019 (Fronzek

65   et al., 2018; Ruiz-Ramos et al., 2018; Snyder et al., 2019). These three studies sample multiple perturbations to temperature and precipitation, and two of the three add CO_2 as well, for a total of 132, 99, and 220 different combinations, respectively. All take advantage of the structured training set to construct emulators ("response surfaces") of climatological mean yields, omitting year-to-year variations. All the 2018–2019 papers have some limitations, however, for assessing global agricultural impacts, including that none evaluate responses in every grid cell globally. Two involve many crop models but only one crop

70   (wheat) (Fronzek et al., 2018; Ruiz-Ramos et al., 2018) and cover only 1–4 individual sites. Snyder et al. (2019) analyzes five crops over ∼1000 sites with individual site-specific crop models, and extrapolates in space to estimate mean latitudinal responses.

In this paper we describe a set of globally-gridded crop model emulators developed from the new parameter-sweep dataset of the Global Gridded Crop Model Intercomparison (GGCMI) Phase II effort. GGCMI Phase II, a part of the Agricultural Model

75   Intercomparison and Improvement Project (AgMIP) (Rosenzweig et al., 2013, 2014), provides the first near-global-coverage systematic parameter sweep of multi-model crop simulations consisting of up to 756 combinations in CO_2, temperature, water

supply, applied nitrogen, and two different assumptions on growing season adaptation ("A0": none and "A1": retaining growing season length) (CTWN-A, Franke et al., 2019; Minoli et al., 2019). The experiment is designed to allow diagnosing the impacts on crop yields of both individual factors and their joint effects, and to allow construction of crop model emulators. In the following, we describe the training dataset (Section 2), the statistical model used for emulation (Section 3), measures of emulator fidelity (Section 4), and examples of preliminary results (Section 5).

2 Training dataset

2.1 The GGCMI Phase II dataset

Table 1. Crop models included in GGCMI Phase II emulators and the number of CTWN-A (Carbon, Temperature, Water, Nitrogen, Adaptation) simulations performed for each model. The maximum number is 756 for A0 (no adaptation) experiments, and 648 for A1 (maintaining growing length) experiments, since T0 is not simulated under A1. "N-Dim." indicates whether the models are able to represent varying nitrogen levels. Each model provides the same set of CTWN simulations across all its modeled crops, but some models omit individual crops. Table adapted from Franke et al. (2019). For clarity, three simulation models included in Phase II are not shown here, those that provided a training set too small to be used in emulation.

Model (Key Citations)	Maize	Soybean	Rice	Winter wheat	Spring wheat	N dim.	Sims per crop (A0 / A1)
CARAIB, Dury et al. (2011); Pirttioja et al. (2015)	X	X	X	X	X	–	**252 / 216**
EPIC-TAMU, Izaurralde et al. (2006)	X	X	X	X	X	X	**756 / 648**
JULES, Osborne et al. (2015); Williams and Falloon (2015); Williams et al. (2017)	X	X	X	–	X	–	**252 / 0**
GEPIC, Liu et al. (2007); Folberth et al. (2012)	X	X	X	X	X	X	430 / 181
LPJ-GUESS, Lindeskog et al. (2013); Olin et al. (2015)	X	–	–	X	X	X	**756 / 648**
LPJmL, von Bloh et al. (2018)	X	X	X	X	X	X	**756 / 648**
pDSSAT, Elliott et al. (2014); Jones et al. (2003)	X	X	X	X	X	X	**756 / 648**
PEPIC, Liu et al. (2016b, c)	X	X	X	X	X	X	149 / 121
PROMET, Hank et al. (2015); Mauser et al. (2015); Zabel et al. (2019)	X	X	X	X	X	–	261 / 232

Table 2. GGCMI Phase II input levels for the parameter sweep. Values for temperature and water supply are perturbations from the historical climatology. For water supply, perturbations are fractional changes to historical precipitation, except in the irrigated (W_∞) simulations, which are all performed with the maximum beneficial levels of water. Bold font indicates the 'baseline' historical level. The full protocol samples across all parameter combinations for a total of 756 cases. Table repeated from Franke et al. (2019).

Input variable	Tested range	Unit
$[CO_2]$ (C)	**360**, 510, 660, 810	ppm
Temperature (T)	-1, **0**, 1, 2, 3, 4, 6	°C
Precipitation (W)	-50, -30, -20, -10, **0**, 10, 20, 30, (and W_∞)	%
Applied nitrogen (N)	10, 60, **200**	kg ha^{-1}
Adaptation (A)	**A0: none**, A1: new cultivar to maintain original growing season length	-

The GGCMI Phase II simulations are described in detail in Franke et al. (2019), but we summarize briefly here. The experiment involves nine different globally gridded crop models, each simulating multiple crops (maize, rice, soybean, and spring and winter wheat) across a systematic parameter sweep of as many as 756 combinations, each driven by a historical climate timeseries with systematic perturbations to CO_2, temperature, water supply, and nitrogen application (CTWN). The simulation protocol involves 4 levels of atmospheric CO_2, 7 of temperature, 9 of water supply, and 3 of applied nitrogen, and simulations are repeated for two adaptation scenarios: "A0" simulations assume no adaptation in cultivar choice, so that growing seasons shorten in warmer climates, and "A1" simulations assume that adaptation in cultivar choice maintains fixed growing seasons. The complete protocol for each modeling group involves up to 43,524 years of global simulated output for each crop. Because the computational demand is high, modeling groups were allowed to submit at various specified levels of participation, with the lowest recommended level of participation consisting of 20% of the maximum possible simulations. The mean participation level is 65%, but three models (APSIM-UGOE, EPIC-IIASA, and ORCHIDEE-crop) contributed data below the recommended threshold ($< 5\%$ of the full protocol) and are excluded here since they could not be robustly emulated. Table 1 shows the participating models and the number of simulation scenarios that each provides, and Supplemental Figure S1 shows model sampling density. Table 2 shows the specified input values; we sample across all parameter combinations.

Each individual crop model simulation is run for 31 years over historic weather for the period of 1981-2010, with added uniform perturbations to any of the CTWN variables. Historical weather is taken for most models from the AgMERRA (Ruane et al., 2015) historical daily climate data product, but the PROMET model uses the ERA-Interim reanalysis (Dee et al., 2011) and the JULES model uses a bias-corrected version of ERA-Interim, WFDEI (WATCH-Forcing-Data-ERA-Interim, Weedon et al., 2014) as these groups have specific sub-daily input data requirements. Temperature perturbations are applied as additive mean shifts, water supply as fractional multipliers to precipitation (except in the irrigated W_∞ case), and CO_2 and nitrogen

application levels are specified as fixed values. Models provide near-global output at 0.5 degree latitude and longitude resolution
105   for each simulation year, including areas not currently cultivated. In analyses where we distinguish yields over currently
cultivated land, we use the masks of Portmann et al. (2010). (See Supplemental Figure S2 for maps of cultivated area.)

2.2 Climatological vs. year-to-year response

We emulate the climatological mean response, because that is the response of interest in assessments of climate change impacts.
The year-to-year response can be significantly different from the forced climatological one, so we do not use information from
110   year-to-year variability but instead emulate the aggregated mean yield in each 30-year simulation. Emulation then becomes
relatively straightforward, since changes in time-averaged yields are also considerably smoother than those in year-to-year
yield response.

   In the GGCMI Phase II simulation output dataset, year-to-year responses to weather are often quantitatively distinct from
responses to climatological shifts, with the discrepancy especially strong in wheat and rice. The difference in behavior is
115   illustrated in Figure 1, which shows irrigated and rainfed maize and wheat in representative locations; open circles and black
lines show the climatological mean response, and solid circles and colored lines the responses for the 30 individual years in
individual scenarios. When discrepancies are large, year-to-year responses are generally stronger than climatological ones, but
exact responses differ by crop and region and even by model within GGCMI Phase II.

   While differences in responses at different timescales can arise for many reasons, including memory in the crop model or
120   lurking covariates, the most likely explanation here is that the regressors used, mean growing-season temperature or precip-
itation, do not fully describe the conditions that affect crop yields. The mean growing-season value is only a proxy for the
distribution of daily climatic conditions that crops are sensitive to, and present-day variations between years can be very differ-
ent from future forced changes. That is, present-day variations in growing-season *means* from year to year may be associated
with changes in growing-season *distributions* that are unrelated to any changes in future warmer climates: a warm year at
125   present may be quite different from a warm year in the future (e.g. Ruane et al., 2016). Changes in temperature distributions
have been shown to strongly affect crop yields (e.g. Hansen and Jones, 2000; Gadgil et al., 2002), though precipitation effects
should be smaller since crops respond not to rainfall but to soil moisture, which integrates over weeks or even months (e.g.
Potter et al., 2005; Glotter et al., 2014; Challinor et al., 2004).

   A second factor of importance is that any nonlinearity in crop responses will itself lead to a distinction between climato-
130   logical and year-to-year fits, even if distributional differences are negligible. Given the interannual variations in the climate
timeseries, the mean annual yield response to a perturbation is not the same as the response of the climatological mean yield.
The effect of nonlinearity may be particularly relevant for precipitation, since model crop yields drop steeply and nonlinearly
with increasing dryness. (Crop yields should drop under excess precipitation as well, but process-based models do not capture
losses in saturated conditions well (Glotter et al., 2015; Li et al., 2019).)

135   In the GGCMI Phase II experiment, the imposed perturbations involve no changes in underlying distributions. The choice
is reasonable, since climate models do not agree on distributional changes. Most models do project small mean increases in
growing-season temperature variability in cultivated areas, and can produce substantial local changes, but models disagree on
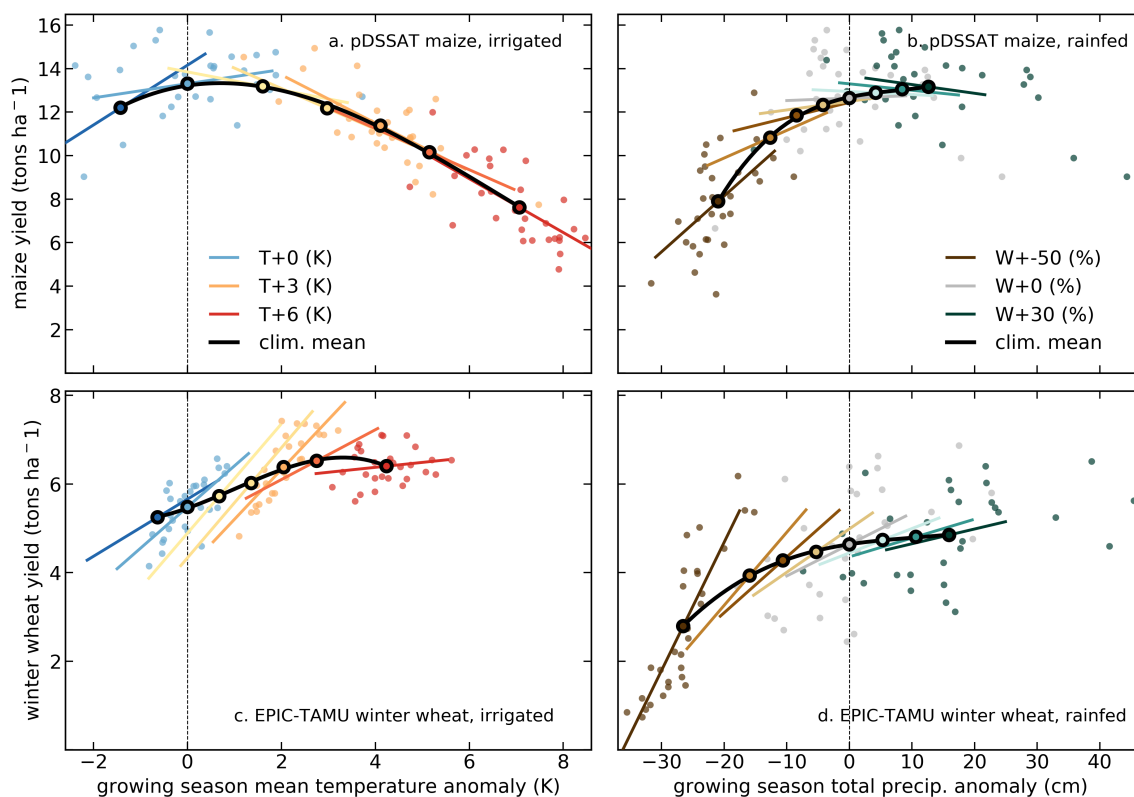
Figure 1. Example showing distinction between crop yield responses to year-to-year and climatological mean shifts in climate variables, showing representative high-yield regions for maize in pDSSAT (northern Iowa, top row) and winter wheat in EPIC-TAMU (France, bottom row). Left column (**a & c**) shows irrigated crops, all temperature cases with other variables held at baseline values, and right column (**b & d**) shows rainfed crops, all precipitation cases. Figure shows A0 output, in which growing seasons shift under future climate, so local growing-season temperature changes can differ from prescribed uniform offsets: for example, a 6 K applied uniform warming results in a growing season temperature warmer by ∼7 K for maize in Iowa (top right), but by less than 6 K for wheat in France (bottom right). Open black circles mark climatological mean yields and bold black lines show a 3rd order polynomial fit through them. Colored lines show linear regressions (by orthogonal distance regression) through the 30 annual yields of each parameter case. Colored circles show annual yields for selected cases. Differences in slopes of colored and black lines mean that responses to year-to-year fluctuations differ from those to longer-term climate shifts. Differences are generally stronger for wheat (bottom) than maize (top). Note that for rain-fed crops, slope differences in this representation could also result from correlated precipitation and temperature fluctuations in the baseline timeseries, but P-T correlations do not contribute to the effects shown here. Such correlations would complicate emulations based on year-to-year yields but would not necessarily bias them.

spatial patterns. For example, in models of the Coupled Model Intercomparison Project Phase 5 (CMIP-5) archive, in the the high-end RCP (Representative Concentration Pathway) 8.5 climate projections to the year 2100 (Riahi et al., 2011), growing

140   season daily maximum temperature variability over currently cultivated rice areas (weighted by production) increases by 10%

in HadGEM2-ES but only by 0.4% in MIROC-ESM-CHEM. (See Supplemental Section S2.) We therefore explicitly test the assumption that distributional changes are not consequential for climatological mean yields: in Section 4.3, we confirm that an emulator trained on the GGCMI Phase II dataset can successfully reproduce yield changes under a full climate model projection.
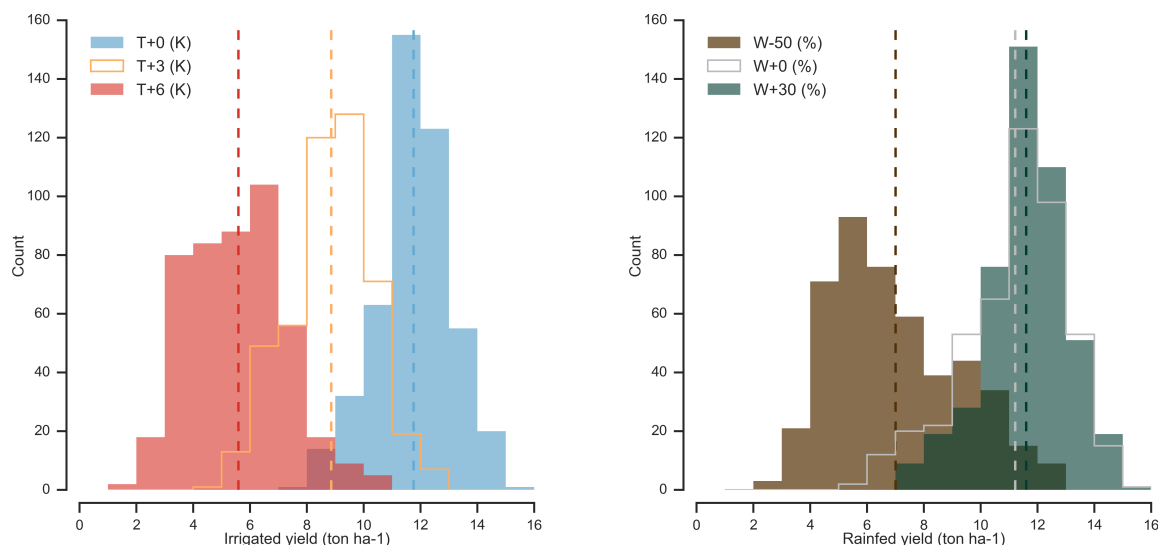
Figure 2. Example showing results of increased crop yield sensitivity to year-to-year climate variations under climate stress. Yield distributions are from examples of Figure 1, top row, of maize in Iowa, (**left**) for irrigated maize in scenarios of altered temperature and (**right**) for rainfed maize in scenarios of altered precipitation. Because yield sensitivities rise under strong warming or drying, distributions of year-to-year crop yields widen in T+6 and P-50% scenarios relative to present-day simulations, even though all input climate timeseries have identical variance for temperature. Note: precipitation changes have different variance since the perturbations are fractional.

145   Note that even though distributions of climate variables are unchanged in the GGCMI Phase II simulations, the spread in annual yields still becomes wider in highly impacted climate states, because of the nonlinearity of yield responses (Figure 2). In the GGCMI Phase II dataset, all crops except rice show greater year-to-year yield variance in conditions of extreme climate stress. (Rice is typically irrigated and experiences no water stress in simulations.) Increased variance has been noted in previous studies. For example, Urban et al. (2012) used statistical models trained on present-day yields to find a projected

150   future increase in yield variance of U.S. maize of 20% per degree K temperature rise. While the authors do not diagnose a specific cause of that increase, they discuss multiple potential mechanisms, including nonlinearity in responses.

3   Emulation

Emulation involves fitting individual regression models from GGCMI Phase II output for each crop and model and 0.5 degree geographic pixel; the regressors are the applied perturbations in CO_2, temperature, water, and nitrogen (CTWN). We discuss

155   here largely emulations of climatological mean crop yields with no growing season adaptation (A0 scenarios), but note that

any output of the crop models can potentially be emulated. We provide separate emulations of irrigated and rainfed yields and applied irrigation water (pirrww in mm yr^{-1}) in both A0 and A1 scenarios, meaning that each model and crop combination results in six sets of regressions. See Supplemental Material Sections 3, 4, and 6 for these additional emulation cases.

3.1 Statistical model

160 For the statistical model of crop yields as a function of CTWN, we choose a relatively simple parametric model with a 3rd-order polynomial basis function. If the climatological mean response is relatively smooth, then a simpler form provides a reasonable fit that allows for some interpretation of resultant parameter weights. A relativity simple parametric form also allows fast model emulation at the grid cell level, rather than requiring spatial aggregation. Emulating at the grid cell level preserves the spatial resolution of the parent models, and means that emulators indirectly includes any yield response to geographically distributed
165 factors such as soil type, insolation, and the baseline climate.

The 3rd-order polynomial CTWN model contains 34 terms (Equation 1), since the N^3 term is omitted, as it cannot be fitted in a training set sampling only three nitrogen levels. To facilitate comparing emulators parameter by parameter, we hold this functional form across locations, crops, and models, other than several necessary distinctions: regressions for irrigated crops do not contain W terms, and regressions for models that do not sample the nitrogen levels omit the N terms.

$$
\begin{aligned}
170 \quad Y = K_1 \qquad\qquad\qquad\qquad\qquad\qquad\qquad\qquad\qquad\qquad\qquad (1)\\
+ K_2 C + K_3 T + K_4 W + K_5 N + K_6 C^2\\
+ K_7 CT + K_8 CW + K_9 CN + K_{10} T^2 + K_{11} TW\\
+ K_{12} TN + K_{13} W^2 + K_{14} WN + K_{15} N^2\\
+ K_{16} C^3 + K_{17} C^2 T + K_{18} C^2 W + K_{19} C^2 N\\
175 \quad + K_{20} CT^2 + K_{21} CTW + K_{22} CTN + K_{23} CW^2\\
+ K_{24} CWN + K_{25} CN^2 + K_{26} T^3 + K_{27} T^2 W\\
+ K_{28} T^2 N + K_{29} TW^2 + K_{30} TWN + K_{31} TN^2\\
+ K_{32} W^3 + K_{33} W^2 N + K_{34} WN^2 + K_* N^3
\end{aligned}
$$

Results shown throughout the paper use this full specification, but we also investigate (in Section 3.2 below) whether some
180 terms can be dropped without significant reduction in emulator fidelity. In general, both higher-order and interaction terms are expected to be important for representing crop yields. Higher order terms are needed because crop yield responses to weather are well-documented to be nonlinear: e.g. Schlenker and Roberts (2009) for T perturbations and He et al. (2016) for W (precipitation). Interaction terms are needed since the yield response is expected to depend on interactions between the major inputs. For example, Lobell and Field (2007) and Tebaldi and Lobell (2008) showed that in real-world yields (with C and N
185 fixed), the joint distribution in T and W is needed to explain observed yield variance. Other observation-based studies have shown the importance of the interaction between W and N (e.g. Aulakh and Malhi, 2005), and between N and C (Osaki et al., 1992; Nakamura et al., 1997).

We do not focus in this study on comparing other functional forms or non-parametric models. Some prior studies have used other statistical specifications in crop model emulation: for example, Blanc and Sultan (2015) and Blanc (2017) use a 39 term
190   fractional polynomial and "borrow information across space" by fitting grid points simultaneously across soil region in a panel regression. The GGCMI Phase II dataset allows fitting our simple 3rd order polynomial form independently at each grid cell while still providing a satisfactory emulation for all models and crops. (See Section 4 for evaluation of the fidelity of emulators constructed with Equation 1.)

3.2 Feature importance and reduced statistical model

195   Because a simpler statistical model may improve the interpretability of its parameter weights, we also develop a reduced version that is satisfactory for most models and crops (Equation 2). To identify terms that can be omitted, we apply a feature selection cross-validation process in which terms in the polynomial are tested for importance. Higher-order and interaction terms are successively added to the regression model, and in each case we calculate an aggregate mean absolute error (weighted by by currently cultivated area) and eliminate those terms that do not contribute significantly to reducing error. The procedure is
200   illustrated in Figure 3. We develop our reduced statistical model by considering yields over currently cultivated land in three models: two that provided the complete set of 672 rainfed simulations, i.e. without the W_∞ simulations, (pDSSAT, EPIC-TAMU), and one that provided the smallest training set (121 input combinations, PEPIC). Although models exhibit different absolute levels of error, all three agree remarkably well on feature importance, i.e. on which terms reduce error and which provide no predictive benefit. (Agreement means that line slopes match in Figure 3.)

205   Results of the feature selection process suggest that 11 terms can be omitted with negligible impact on emulator fidelity, producing the 23-term statistical model of Equation 2.

$$
\begin{aligned}
Y \ = \ & K_1 \\
& + K_2 C + K_3 T + K_4 W + K_5 N + K_6 C^2 \\
& + K_a CT + K_7 CW + K_8 CN + K_9 T^2 + K_{10} TW \\
& + K_{11} TN + K_{12} W^2 + K_{13} WN + K_{14} N^2 \\
& + K_* C^3 + K_* C^2 T + K_* C^2 W + K_* C^2 N \\
& + K_* CT^2 + K_* CTW + K_* CTN + K_* CW^2 \\
& + K_* CWN + K_{15} CN^2 + K_{16} T^3 + K_{17} T^2 W \\
& + K_* T^2 N + K_{18} TW^2 + K_{19} TWN + K_{20} TN^2 \\
& + K_{21} W^3 + K_{22} W^2 N + K_{23} WN^2 + K_* N^3
\end{aligned}
\tag{2}
$$

The eliminated terms include many of those in C: the cubic; the CT, CTN, CTW, and CWN interaction terms; and all higher order interaction terms in C. Finally, we eliminate one 2nd-order interaction term in W and two in T. Implications of this choice include that nitrogen interactions are complex and important, and that water interaction effects are more nonlinear than those in temperature. Note that some terms that did not reduce the aggregate error must still be included if a higher order version
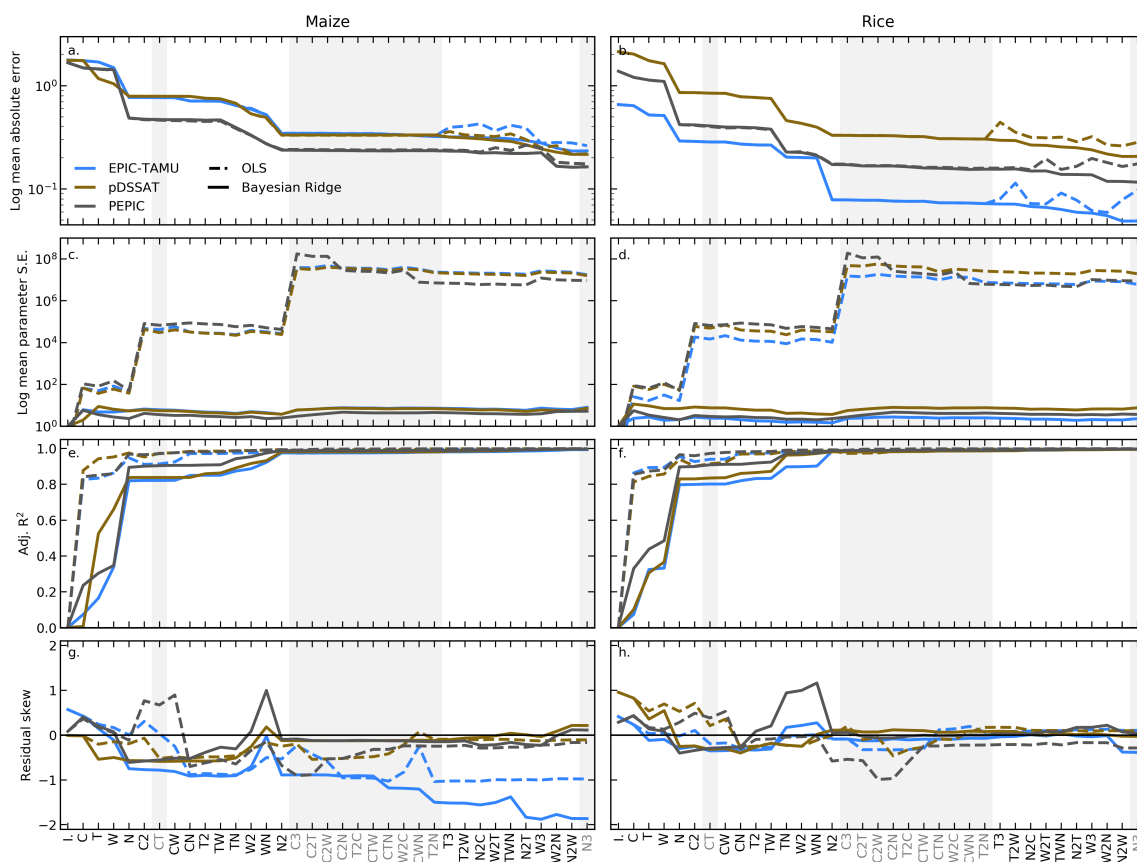
Figure 3. Illustration of results from the polynomial feature selection process for three different crop models (colors), for all grid cells with more than 1000 ha cultivated for maize (**left**) and rice (**right**). Solid lines are Bayesian Ridge regression results and dashed lines those for standard OLS. Rows show four metrics of fit quality and x axes the terms successively tested in the statistical model, sequentially added to the model in order from left to right. Terms that do not reduce the aggregate error are marked in gray and are not included in the final model. **a & b:** log mean absolute error between emulated yield and simulated values calculated with a three fold cross validation process, where the emulator is trained on two thirds of the data and predicts the remaining third. **c & d:** log mean standard parameter error. The Bayesian Ridge method strongly reduces parameter error and results in more stable estimates. **e & f:** adjusted R^2 score for the fit at each model specification. **g & h:** distribution of the residuals. Skewness is low at the high model specifications tested in all model cases other than EPIC-TAMU maize.

220 of that term provides benefit: for example, including the T^3 term requires also retaining T^2 and T terms. The reduced-form emulator is acceptable across currently cultivated land for all model and crop combinations other than JULES soy and spring wheat and PROMET soy and rice. These cases involve yield responses that benefit strongly from inclusion of higher order carbon interaction terms. Additional terms in the statistical model also help emulation in some geographic locations outside of currently cultivated regions, where yield responses are often non-standard. (See Supplemental Material Section 7 for evaluation

225 of the fidelity of emulators constructed with Equation 2 and for more details on JULES and PROMET.)

3.3 Model fitting

To fit the parameters K, we use a Bayesian Ridge regularization method (MacKay, 1991) rather than standard ordinary least squares (OLS). The Bayesian Ridge method reduces volatility in parameter estimates when the sampling is sparse, by weighting parameter estimates towards zero, allowing the use of a consistent functional form across all models and locations. The choice

230   slightly reduces mean absolute error for some of the high-order interaction terms in the model (Figure 3, top row) but drastically reduces standard parameter error in the model by stabilizing the estimates (Figure 3, third row). The estimation method scores relatively lower on adjusted R^2 for the simplest parameter specifications, but quickly reaches parity with the OLS. We use adjusted R^2 as a metric because additional terms are penalized (Equation 3, where n is the number of samples and k is the number of features):

235    $$R^2_{adj} = 1 - \frac{(n-1) \cdot (1 - R^2)}{n - k} \qquad (3)$$

We use the implementation of the Bayesian Ridge estimator from the scikit-learn package in Python (Pedregosa et al., 2011).

An additional diagnostic of fit quality is the distribution of residuals: normally or near-normally distributed residuals imply that errors around the fit are random and unbiased. When fitting Equation 1 to the GGCMI Phase II dataset, the distribution of the residuals depends on the number of features included in the regression, the method for estimating the parameters, and the

240   target distribution in the training set. The residuals are only normally distributed (pvalue > 0.05 in the Shapiro–Wilk test) for a single model, PEPIC, for any specification tested here, but their skew is relatively small except in a single case, EPIC-TAMU maize (Figure 3, fourth row). While including higher-order terms in the statistical model generally reduces residual skew, for EPIC-TAMU maize it increases skew instead, but also reduces the error in cross-validation, which we consider more important in the context of emulation. The residual distribution suggests that projections using the EPIC-TAMU maize emulator will tend

245   to be biased high, but in practice the overall magnitude of these errors is below 2% of yield changes. (See Section 4.2.)

4 Emulator evaluation

In this section we show illustrations of GGCMI model yield responses to climate perturbations and evaluate the ability of our emulators to reproduce them. Model emulation with the parametric method used here requires that crop yield responses be sufficiently smooth and continuous to allow fitting with a relatively simple functional form; in Section 4.1 we show that

250   this condition largely holds in the GGCMI Phase II simulations. In section 4.2 we evaluate metrics of emulator performance and show that emulation errors – discrepancies between emulation and simulation – are generally small, especially when compared to the differences across crop models or to projected yield changes. Emulation errors become problematic only in certain, limited geographic locations, usually where crops are not currently grown. We analyze here results using the 34-term polynomial of Equation 1; see Supplemental Material Section 7 for analogous analysis of the 23-term polynomial of Equation

255   2. Finally, in Section 4.3, we assess the emulator's ability to reproduce crop yields in a more realistic future simulation driven by a climate model projection, and find that any effects of changes in climate variability not included in the GGCMI Phase II training set are generally small relative to the effects of mean changes.

4.1 Yield response

Crop yields show strong spatial differentiation across geographic regions, and emulators are able to readily reproduce these.
260 Figure 4 illustrates the spatial yield pattern under current climate for one crop and model (maize in LPJmL). Absolute emulation errors are low – 99.8% of grid cells have errors below 0.5 tons ha^{-1} – but emulation errors as a percentage of baseline yield can be large in areas with low potential yield and no current cultivation in the real world (e.g. the Sahara, Patagonia). These regions are not currently viable for agriculture and may never become viable even under extreme climate change. Emulator spatial skill varies across models and crops, with maize being the quantitatively easiest to emulate across all models and locations.
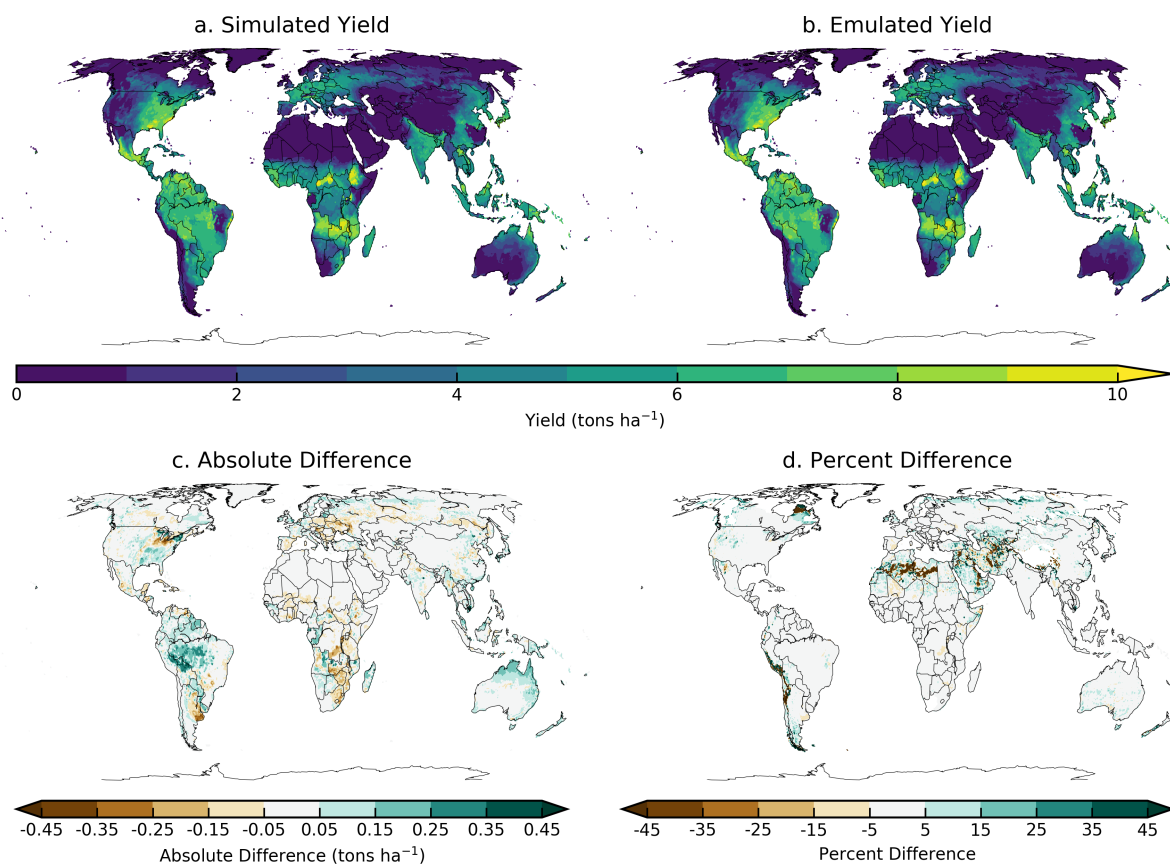
Figure 4. Illustration of spatial pattern in baseline yield successfully captured by the emulator: simulated (**a.**) and emulated (**b.**) yield under historical (1981-2010) conditions for rainfed maize from the LPJmL model. Absolute yield differences (**c.**) are less than 0.5 ton ha^{-1} in almost all (99.8%) grid cells across the globe. Percent difference (from simulated baseline, **d.**) is below 5% in most (75%) grid cells currently cultivated in the real world. Approximately 7% of all grid cells, but only 3% of currently cultivated grid cell, have emulated yields that differ from the baseline simulation by more than 20%. Notable exceptions include areas with very low simulated baseline yield, including for example the Sahara, the Andes, and northern Quebec. Percent error weighted by cultivation area globally is essentially zero (see also Table 3). Performance varies by crop and model. See Supplemental Figures in Section 8 for more examples.
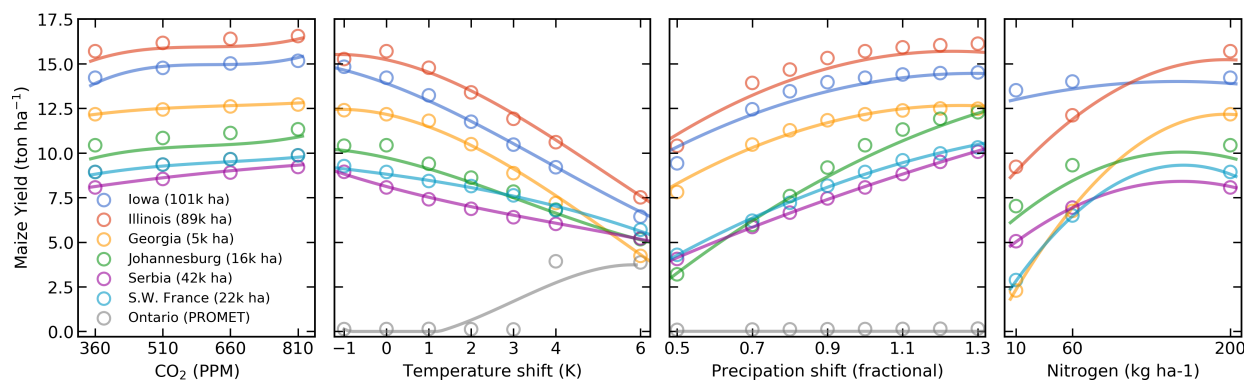
Figure 5. Illustration of spatial variations in yield response, which are successfully captured by the emulator. Panels show simulations (points) and emulations (lines) of rainfed maize in the pDSSAT model in six example locations selected to represent high-cultivation areas around the globe. Legend includes hectares cultivated in each selected grid cell. Each panel shows variation along a single variable, with others held at baseline values. Dots show climatological mean yields and lines the results of the full 4D emulator of Equation 1. In general the climatological response surface is sufficiently smooth that it can be represented within the sampled variable space by the simple polynomial used in this work. In some cases extrapolation would produce misleading results, and the emulator fails in conditions where yield response changes abruptly. Failure is illustrated here by rainfed maize in north-central Ontario for the PROMET model (in gray), which shows present-day yields of zero rising abruptly if temperature warms by 4 degrees.

265   Yield responses to the four main drivers considered here (C, T, W, and N) are also quite diverse across locations, crops, and models, but in nearly all cases the local climatological mean responses are smooth enough to permit emulation with the functional form used here. Figure 5 illustrates the geographic diversity of responses within a single crop and model, for rainfed maize in pDSSAT. While the CO_2 responses (in ton ha^{-1}/ppm) are quite similar, the precipitation response is stronger in more arid locations and the nitrogen responses appear strongly location-dependent. The heterogeneity in response supports the

270   choice of emulating at the grid cell level. In regions with current cultivation, yields evolve smoothly across the space sampled, and the polynomial fit captures the climatological-mean response to perturbations well. Emulators do perform poorly in a few regions that involve discontinuous or irregular yield responses. Poor performance is illustrated here with PROMET maize in northern Canada, which is too cold for maize at present in PROMET (0 ton ha^{-1} yield), but which shows an abrupt rise to moderate yields once temperature rises by 4 degrees. Under these conditions, the 3rd order polynomial cannot fit the response,

275   and errors are high. See Section 4.2 for additional discussion.

Crop yield responses in all models generally follow similar functional forms at any given location, though with a spread in magnitude (Figure 6, which shows rainfed maize in northern Iowa in a selection of GGCMI models). Absolute yield differences between models can be substantial because some models are uncalibrated. In general, models are most similar in their responses to temperature perturbations, and least similar to changes in CO_2. That is, CO_2 fertilization effects *within* a single model are

280   consistent across locations, but CO_2 effects differ strongly *across* models.
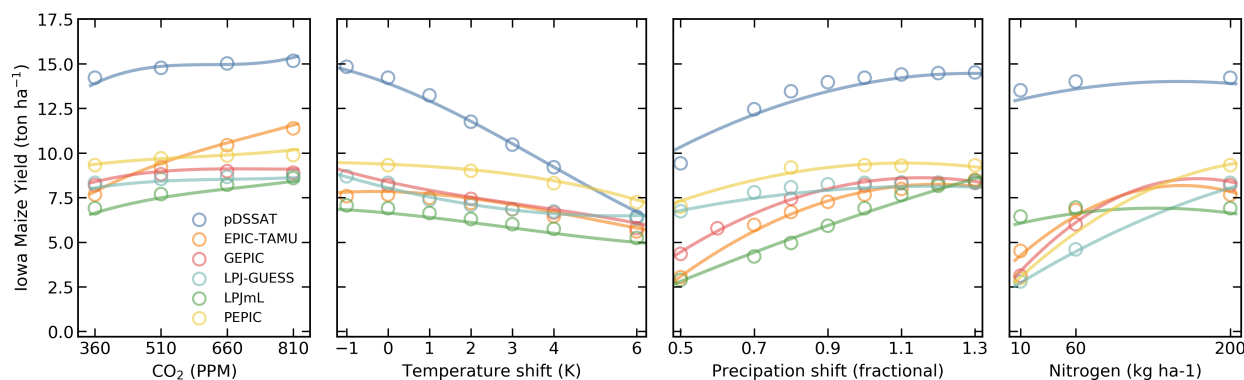
Figure 6. Illustration of variations in yield response across models, again successfully captured by the emulator. Panels show simulations and emulations from six representative GGCMI models for rainfed maize in the same Iowa grid cell shown in Figure 5, with the same plot conventions. Three models (PROMET, JULES, and CARAIB) that do not simulate the nitrogen dimension are omitted for clarity. Models are uncalibrated, producing spread in absolute yields. While most model responses can readily emulated with a simple polynomial, some response surfaces diverge slightly from the polynomial form, producing emulation error (e.g. pDSSAT here, for water), but resulting error generally remains small relative to differences across models.

Note that while the nitrogen dimension is important, it is also the most troublesome to emulate in the GGCMI Phase II experiment because of its limited sampling. The GGCMI Phase II protocol specified only three nitrogen levels (10, 60 and 200 kg N y^{-1} ha^{-1}), so a third-order fit would be over-determined but a second-order fit can result in potentially unphysical results. Steep and nonlinear declines in yield with lower nitrogen levels mean that some regressions imply a peak in yield between the
285   100 and 200 kg N y^{-1} ha^{-1} levels (Figure 6, right). While reduced yields under high nitrogen levels are physically possible and could reflect over-application at particular times in the growing period, they are implausible at the magnitude shown here and likely an artifact of the fit. The Bayesian Ridge estimator mitigates the 'peak-decline effect' in the nitrogen dimension relative to ordinary least squares, but does not entirely remove it. The polynomial fit also cannot capture the well-documented saturation effect of nitrogen application (e.g. Ingestad, 1977) as accurately as would be possible with a non-parametric model.

290   **4.2   Emulator performance metrics**

Our emulators collectively consist of nearly 3 million individual regressions, so developing concise performance metrics poses a challenge. No general agreed-upon criteria exist for defining an acceptable crop model emulator, so we present two different metrics below, one relatively loose and one more stringent. Both metrics assess the ability of the emulator to reproduce simulated crop yields in the GGCMI Phase II experiment. In this section we show only results from emulators based on the 34-term
295   Equation 1; see Supplemental Material Section 7 for analogous assessment of emulators based on the 23-term Equation 2.

    1. Normalized error. We take as our first metric what we term the "normalized error", which compares the fidelity of an emulator to the inter-model spread. For a multi-model comparison exercise like GGCMI Phase II, a reasonable though loose emulator criterion is that its errors be small relative to inter-model differences. The normalized error e is defined separately
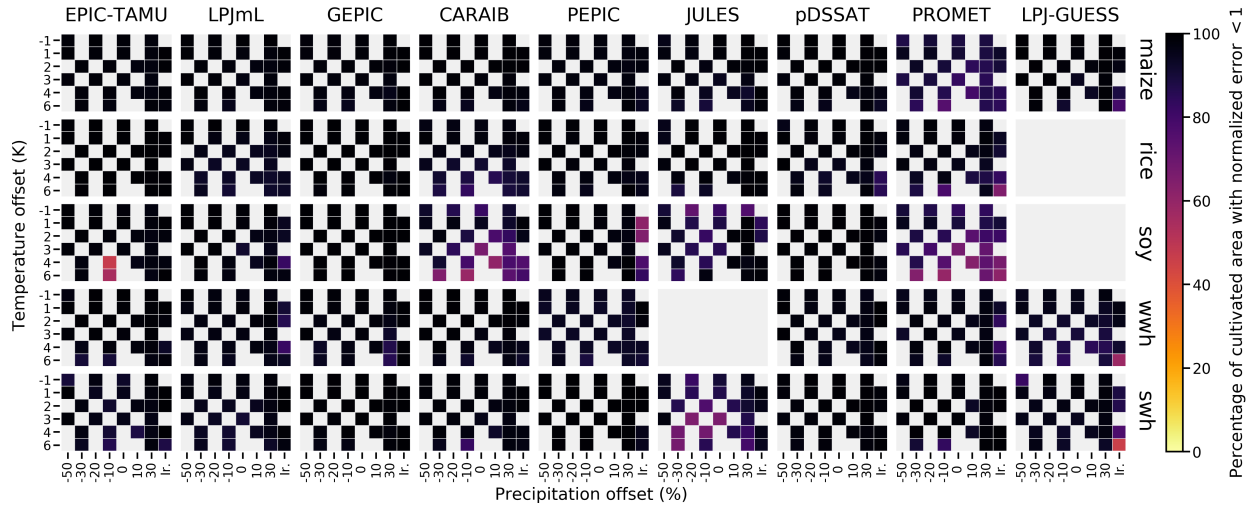
Figure 7. Assessment of emulator performance over currently cultivated areas based on normalized error (Equations 5). We show performance of all 9 models emulated, over all crops and all sampled T and W inputs ("ir." indicates the irrigated W_∞ setting), but with CO_2 and nitrogen held fixed at baseline values. Large columns are crops and large rows models; squares within are T, W scenario pairs. Colors denote the fraction of currently cultivated hectares ("area frac") for each crop with normalized area e less than 1 indicating the the error between the emulation and simulation less than one standard deviation of the ensemble simulation spread. Of the possible 63 scenarios at a single CO_2 and N value, we consider only those for which all 9 (8 for rice, soybean, and winter wheat) models submitted data (Figure S1) so the model ensemble standard deviation can be calculated uniformly in each case. JULES did not simulate winter wheat and LPJ-GUESS did not simulate rice and soybean. Emulator performance is generally satisfactory, with some exceptions. Emulator failures (significant areas of poor performance) occur for individual crop-model combinations, with performance generally degrading for colder and wetter scenarios.

for each C,T,W,N scenario s as the difference between emulated and simulated fractional yield changes, normalized by the
standard deviation in simulated changes across all models:

$$e_s = \frac{F_{em,s} - F_{sim,s}}{\sigma_{sim,s}} \tag{4}$$

where F is the fractional change in yields Y between scenario s and baseline b:

$$F_s = \frac{Y_s - Y_b}{Y_b} \tag{5}$$

We calculate the mean error for each grid cell, model, and crop in each C,T,W,N scenario by comparing emulated and simulated
yields. A normalized error $e < 1$ means that any deviation of the emulation from the simulation is less than 1 standard deviation
of the inter-model spread.

Evaluation of this metric implies that GGCMI Phase II emulators are generally satisfactory. Emulator performance is illustrated in Figure 7, which shows all models and crops crops over currently cultivated area. Over all crops and models, the
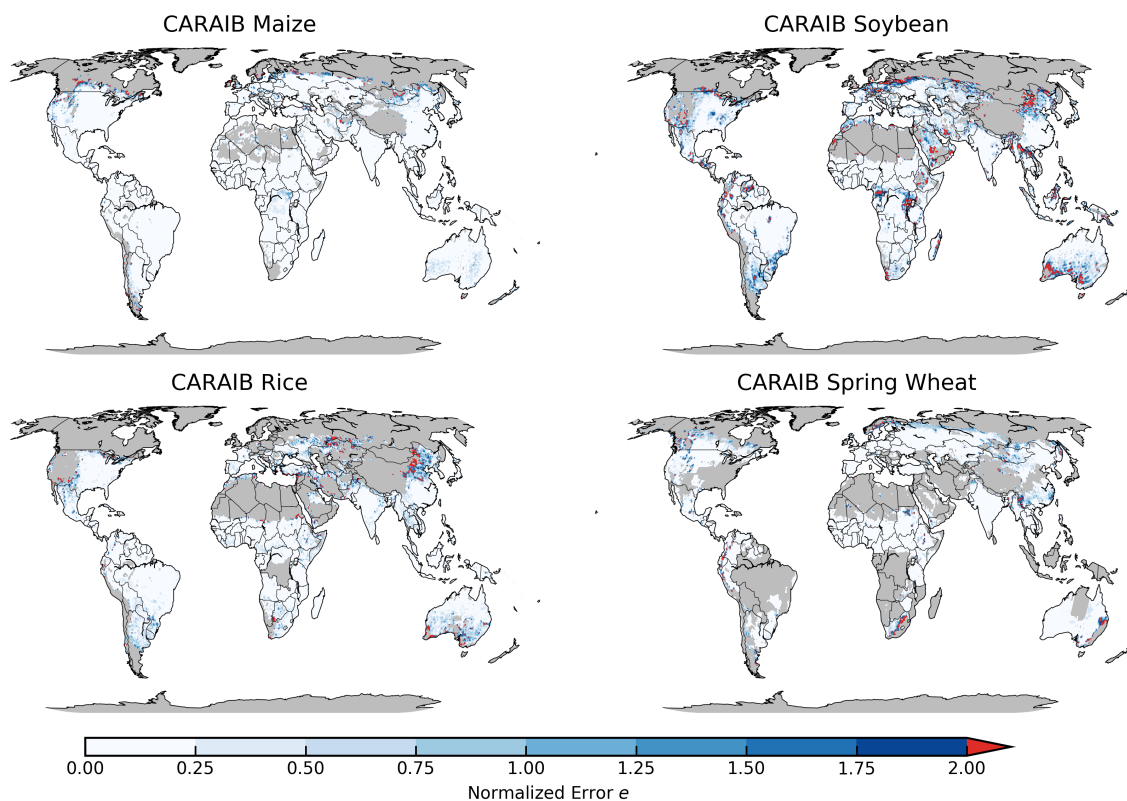
Figure 8. Illustration of our first test of emulator performance, applied to the CARAIB model for the T+4 scenario for rainfed crops. Colors indicate the normalized emulator error e, where $e > 1$ means that emulator error exceeds the multi-model standard deviation. For consistency, we show e only for geographic areas simulated by at least six models and where baseline yields are greater than 0.5 ton ha^{-1}. Emulator performance is generally good relative to model spread in areas where crops are currently cultivated (compare to Figure S2-S3) and in temperate zones in general; emulation issues occur primarily in marginal areas with low yield potentials.

average normalized error $e < 1$ over 95% of currently cultivated area. For maize, the most tractable crop to emulate, all 9 models return $e < 1$ over 97% of currently cultivated area. Only three crop-model combinations are problematic, returning $e < 1$

310 over less than 90% of cultivated area even when using the 34-term statistical model: PROMET and CARAIB for soybeans (79% and 83%), and JULES for spring wheat (85%). Misfits typically occur when models show strong discontinuities in yield response (as shown in Figure 5), or when carbon fertilization gains interact nonlinearly with changes in temperature or water. Including higher-order C terms helps in the latter case but does not reduce emulator errors to zero. See Supplemental Figures S22-S23 for examples of worst-case emulator failures.

315   While Figure 7 shows only currently cultivated land, performance can be worse in locations where crops are not currently cultivated, or on marginal lands where current potential yields are low. (In general, emulator performance is poor anywhere that models show steep yield changes once some threshold has been reached, whether these are abrupt gains or complete crop failures.) Figure 8 illustrates this effect for CARAIB in the T+4 scenario, showing normalized error over all simulated area

with non-zero baseline yield and at least 6 models providing simulations. CARAIB emulator performance is generally good
320 where crops are grown but can be poor ($e > 2$) in arid or mountainous zones, e.g. the edges of the Sahara, Inner Mongolia,
South Africa and Southern Australia. Note that the choice of statistical model for emulation involves a trade-off in the spatial
pattern of errors: adding terms to the statistical model increases emulator fidelity in problematic "fringe" areas where crops are
currently not cultivated, but reduces it slightly over high-yield areas. For example, CARAIB maize emulators have normalized
error $e < 1$ over 98.8% of currently cultivated land with the reduced 23-term Equation 2 but only 98.5% with the 34-term
325 Equation 1. Over simulated uncultivated land, CARAIB maize emulators have $e < 1$ for only 88.7% of area with the reduced
Equation 2 but 93.7% with the full Equation 1.

Note that the normalized error assessment is relatively forgiving for several reasons. First, it is an in-sample validation,
with the emulation evaluated against the simulations actually used to train the emulator. Had we used a spline interpolation,
the error would necessarily be zero. Second, the metric scales emulator fidelity not by the magnitude of yield changes in the
330 evaluated model but by the spread in yield changes across models. The normalized error e for a given model then depends
on the particular suite of other models considered in the intercomparison exercise. The rationale for the choice is to relate the
fidelity of the emulation to the true uncertainty, which we take as the multi-model spread, but the metric then has the property
that where models differ more widely, the standard for emulators becomes less stringent, and vice versa. In GGCMI Phase II
the effect is manifested in the higher normalized errors for soybeans across all models, which result not because soybean yields
335 are difficult to emulate but because models agree more closely on yield changes for soybeans than for the other crops.

2. Out-of-sample validation. We provide a second, more stringent test of emulator performance via a cross validation (also
termed an out-of-sample validation). In this test the GGCMI Phase II dataset is split randomly into two parts, with 90% of the
data used to train the model and the held-out 10% used to test the fidelity of the resulting emulator. We calculate the root mean
square error (RMSE) between emulated (predicted) and actual simulated values across the test set, repeat the process twice,
340 and average the results of the two splits. As a last step, we normalize the RMSE in each grid cell by dividing by the simulated
yield change.

The resulting error metric is generally low. Table 3 shows the yield-change-normalized RMSE for rainfed crops in all models
over currently cultivated land, both in selected major producing regions and in the global average. (We include all simulations
in CTWN space and take the average error value.) Mean grid cell RMSE is below 5% of yield changes in all cases, or in
345 absolute terms less than 0.2 ton ha^{-1} for all except JULES soy, which is 0.36 ton ha^{-1} in the global mean. For irrigated crops,
absolute emulator errors are generally lower, but since irrigated crops experience lower yield changes the fractional errors are
similar. See Supplemental Material Section 9 for maps of cross validation RMSE for each crop and model.

Note that this metric is relatively simple and may be over-conservative. The randomized sampling protocol for dividing
training and test sets can mean that a training set omits edge simulations at the highest or lowest value in CTWN space. The
350 test prediction then involves extrapolating out of the training set range (e.g. predicting a T+6 case when the training set extends
only to T+4), an improper use of an emulator. Values would be lower under a different sampling strategy (e.g. "leave-one-out").
For additional discussion of more detailed potential evaluation metrics, see e.g. Castruccio et al. (2014).

Table 3. RMSE of emulator replication of simulated yields of rainfed crops, stated as a percentage of simulated yield change. Values are the mean grid cell error as a percentage of simulated yield change, over all currently cultivated grid cells weighted by cultivation area, for selected major regions (NA: North America, SA: South America). For comparison, global mean values are show in parentheses. Errors are calculated using the 90-10 cross validation scheme described in text, with the model trained on 90% of the data and validated on the held-out 10% (repeated twice). All fits are made with the Bayesian Ridge method; for context we mark with * those cases where the Bayesian Ridge is required because the OLS linear model fails (e.g. PEPIC, which has the lowest number of samples at n=121).

Model	NA Maize %	SA Soybean %	SE Asian Rice %	NA S. Wheat %	European W. Wheat %
CARAIB	0.7 (0.9)	2.4 (2.4)	2.4 (2.4)	1.3 (1.4)	2.7 (1.9)
EPIC-TAMU	2.4 (1.8)	1.8 (2.6)	1.6 (1.6)	1.8 (1.9)*	1.1 (1.1)
JULES	2.6 (2.6)	4.6 (4.0)	1.6 (1.7)	2.0 (2.2)	NA
GEPIC	2.1 (2.4)	1.0 (1.2)	2.0 (2.1)	3.7 (3.3)	4.0 (2.9)
LPJ-GUESS	1.0 (1.1)	NA	NA	1.0 (1.3)	1.0 (1.2)
LPJmL	1.8 (1.8)	1.1 (1.3)	1.2 (1.1)	0.8 (1.1)	1.5 (1.3)
pDSSAT	1.9 (1.7)	1.2 (1.1)	1.7 (1.6)	1.1 (1.3)	1.4 (1.5)
PROMET	3.4 (2.7)*	2.0 (2.7)*	2.1 (1.8)*	4.3 (3.7)*	4.6 (3.4)*
PEPIC	1.8 (1.8)*	1.4 (1.9)*	1.4 (1.4)*	2.3 (2.3)*	4.9 (2.9)*

4.3 Emulation of realistic climate projections

Finally, we test the ability of an emulator based on the GGCMI Phase II perturbed mean training set to reproduce the response
355 of a crop model driven by a realistic evolving climate scenario. The goal is to assess whether effects of future changes in temperature and precipitation distributions are strong enough to compromise an emulator based on the GGCMI Phase II dataset. We first drive the LPJmL crop model (representative of GGCMI models) with climate model output under the high-end RCP 8.5 scenario. We choose for this purpose a climate model (HadGEM2-ES) with relatively large changes in growing-season temperature variability (Supplemental Table S1) among members of the Coupled Model Intercomparison Project Phase
360 5 (CMIP-5) archive (Jones et al., 2011; Martin et al., 2011; Taylor et al., 2012). We then drive the LPJmL emulator with the HadGEM2-ES yearly-growing season anomalies, and evaluate how well the resulting emulated yields reproduce those simulated under the full climate scenario. The comparison suggests that globally, the results of future distributional shifts on climatological yields are small relative to the effects of mean changes (Figure 9). In the LPJmL example of Figure 9, emulated and simulated global production in the last decade of the simulation are identical to within 1.5% for all crops. Emulators
365 also reproduce decadal variations in yields, which are especially strong in spring wheat grown in northern latitudes, and even capture much of the residual year-to-year yield variability. (R^2 of emulated vs. simulated annual yield anomalies relative to the 10-year running mean is 0.8 for spring wheat and ∼0.3 for all other crops.)

Distributional effects might be expected to be stronger at high latitudes, because temperature and precipitation variability are larger there, so that changes in variability can be correspondingly more important. However, most crops (spring wheat, winter
370 wheat, and maize) show no emulator bias that grows with latitude. Rice is the exception: the climatological-mean emulator
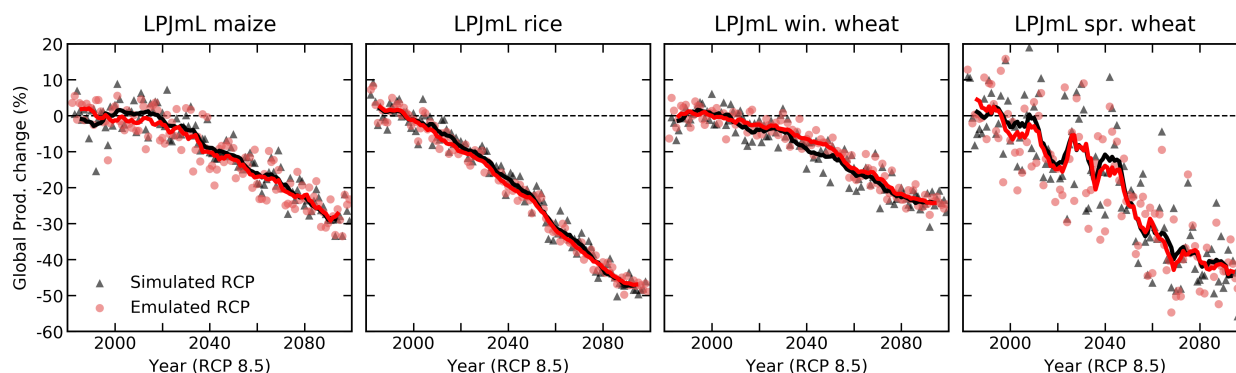
Figure 9. Test of emulator performance in reproducing yield simulations made with a realistic climate projection. Panels show simulated (black) and emulated (red) global production for four crops from the LPJmL model, driven with temperature and precipitation outputs from the HadGEM2-ES climate model for the RCP8.5 scenario. In both cases nitrogen and CO_2 are held fixed, at 200 kg ha^{-1} and 360 ppm. Points show yearly global production change from the 1981-2010 baseline, and lines show a 10-year running mean. See text for discussion of relating the HadGEM2-ES temperature timeseries to the appropriate offset used in emulation. Emulators trained on uniform climatological offsets reproduce well the simulated production response under a realistic climate scenario: yields at end of century match to within 1.5%.

slightly over-predicts yield losses in the tropics and under-predicts losses at higher latitudes (where little rice is currently grown). Poleward of 30 degrees latitude, the LPJmL simulation under the HadGEM2 RCP scenario shows a 49% reduction in rice yields by end-of-century (without growing-season adaptation), but the GGCMI-based emulator produces a reduction of only 39% (Supplemental Figure S11). These losses are concentrated in the lower mid-latitudes: only 21% of global rice is
375   cultivated poleward of 30 degrees, and only 1% poleward of 45 degrees.

It is worth noting two complications involved in comparing emulated to simulated yields under a realistic climate change scenario, as in Figure 9. First, it is not trivial to choose how to relate temperature or precipitation in the evolving climate scenario to the T and P offsets used as regressors to the emulator. Using growing-season mean temperature can lead to complications if crop models assume that growing season lengths shift under climate change. For consistency, we match the temperature
380   changes in the climate scenario to their equivalent emulator regressors by calculating means over the fixed baseline growing season. This choice ensures that the emulation is appropriately matched to the simulation. Second, while the emulator outputs an estimated yield change, the baseline from which that yield change is calculated will be different between simulation and emulation, because the historical climate timeseries are not identical. For example, the baseline (1981-2010) yield of winter wheat simulated by LPJmL using the AgMERRA timeseries as part of GGCMI Phase II is 7% lower than that simulated using
385   the HadGEM2-ES timeseries. To minimize the effects of different historical climate assumptions, we drive the emulator with the anomaly of the climate scenario from its own 1981-2010 mean. Bias in the historical climate timeseries could in theory produce discrepancies between emulated and simulated yield changes because of the nonlinearities discussed in Section 2.2, but the effect appears to play little role in the LPJmL comparison of Figure 9.

5 Emulator results and products
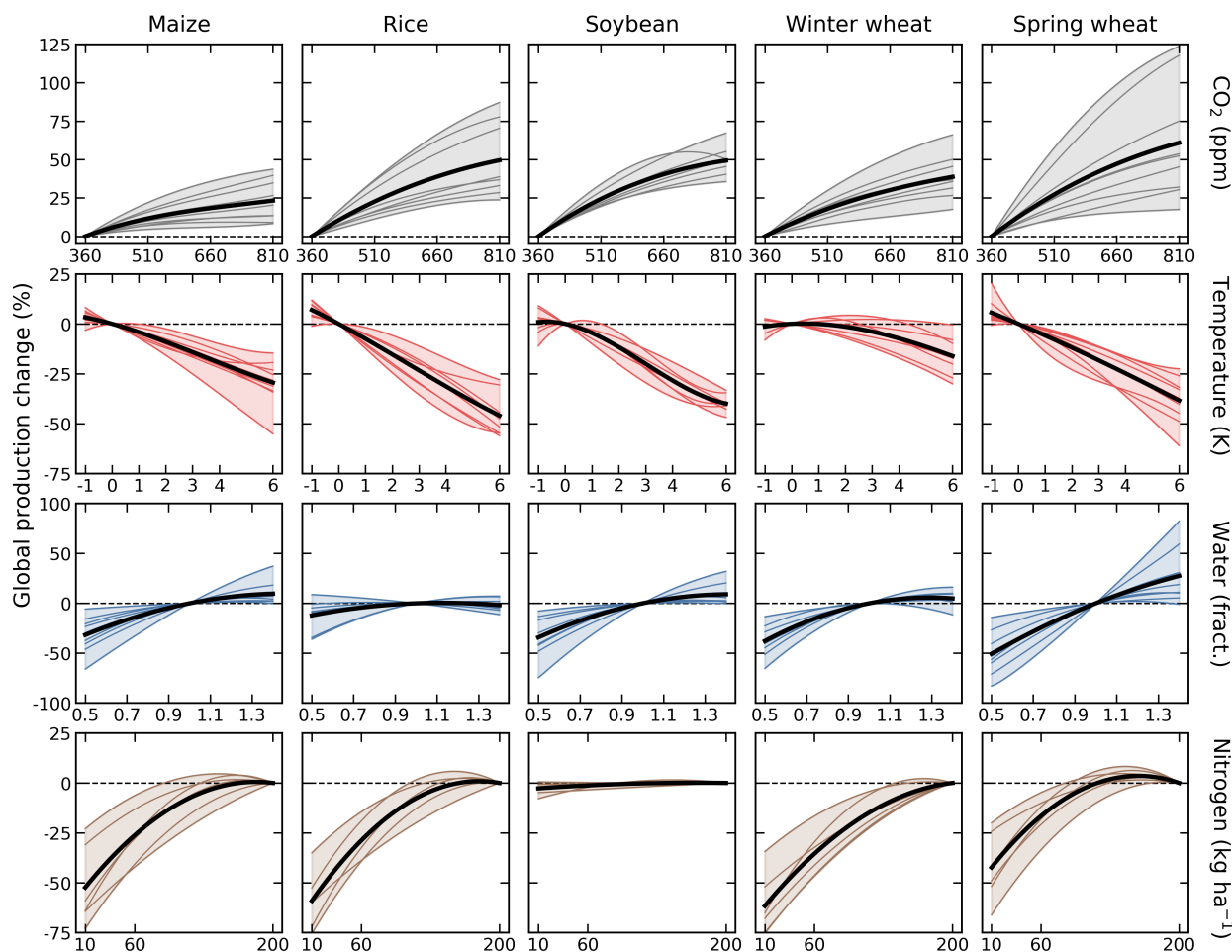
Figure 10. Emulated global damage functions for the five GCCMI Phase II crops over the four CTWN dimensions varied. Black line shows the multi-model mean and shaded area and colored lines the individual models. Each panel shows response to one covariate for rainfed crops, with all others held constant at baseline values (e.g. C = 360 ppm, N = 200 kg ha^{-1}). Damages are reported as percent change in global production over currently cultivated land relative to the 1981-2010 baseline. Note that y-axis ranges are not uniform. As expected, the N response is smallest in soybeans, which are nitrogen fixers, and the C response smallest in maize, which is a C4 crop. See Supplemental Figure S12 for an analogous figure identifying each crop model, and Supplemental Figure S13 for damage functions for the A1 (adpative growing season) emulators, which have reduced temperature responses.

390   The crop model emulators developed here can be used for a variety of applications, because the emulator transforms the discrete simulation samples into a continuous response surface at any geographic scale. One use is construction of continuous agricultural damage functions in a flexible format. As an example, we present in Figure 10 global damage functions over each of the four dimensions tested in this study, constructed from the 4D emulation of each crop model.

These damage functions are useful in diagnosing commonalities and differences in the responses of crop models. In most
395 cases, models agree on the sign of responses to individual factors, but the spread in model responses is comparable to the
median response. Inter-model spreads are largest for spring wheat and smallest for soybeans, as also shown in Figure 7. Model
responses to individual factors conform to expectations. As expected, the CO_2 response is smallest for maize, which is a C4
grass, and the nitrogen response is smallest for soybeans, which are efficient fixers of atmospheric nitrogen. Nitrogen responses
in crops other than soybeans are relatively similar, and most models show saturation beginning at values less than $200 \, \mathrm{kg \, ha^{-1}}$.
400 In nearly all crop models and for all crops except spring wheat, damages from reduced precipitation exceed benefits from
increased precipitation. Spring wheat is the exception, likely because it is grown in high latitudes where rainfall may be
limiting. Rice, by contrast, which is generally grown in locations with abundant water, shows nearly no benefit from increased
precipitation. Note that these damage functions do not consider whether increased precipitation might permit cultivation in
new areas, and also that crop models generally do represent damages from excess soil moisture well (Li et al., 2019).

405 The GGCMI Phase II emulators are also intended as a tool for impacts assessments. The T and W functions presented in
Figure 10 are not true global projections, because they emulate the consequences of uniform shifts across the globe. However,
the emulator allows building analogous damage functions based on climate model output, which has more realistic spatial
patterns of changes in temperature and precipitation. In Figure 11, we show emulated maize responses for 3 crop models
under the RCP8.5 scenario, using output from 5 climate models from the CMIP-5 archive. Losses are shown as a function of
410 mean growing-season temperature over currently cultivated land. While these damages functions aggregate over all currently
cultivated land, the global coverage of GGCMI Phase II allows impacts modelers to develop damage functions for any desired
geopolitical or geographic region larger than 0.5 degrees in latitude and longitude.

The emulated responses of Figure 11 allow diagnosing the factors of greatest importance to projected yield changes under
future climate change. In the maize example here, temperature is the overwhelmingly dominant factor for pDSSAT, but CO_2
415 responses are far larger in PROMET. (CO_2 is important across models for spring wheat, see Figure S14.) For all crop models,
the aggregated effects of precipitation changes are negative, exacerbating yield losses (compare T and T+W cases), because
precipitation in HadGEM2 actually declines over maize cultivation regions, especially in Central and S. America. Precipitation
effects are relatively small, however, as manifested in two ways: as only a small mean shift in yield projections for individual
crop models (compare T and T+W cases), and as a relatively small increase in the spread of points here at a given temperature,
420 despite the fact that the climate projections used involve different relationships between temperature and precipitation change.
By contrast, the carbon fertilization response for PROMET is so large that projections from climate models of different sen-
sitivities ($\Delta T/\Delta CO_2$) become clearly separated in Figure 11. PROMET yield responses would be more similar if plotted as a
function of CO_2 than they are when plotted as in Figure 11 as a function of temperature change.

Disaggregating the factors driving crop yield changes also highlights the fact that errors of emulation are much smaller than
425 the spread across crop models or even across different climate simulations. PROMET is the most quantitatively difficult model
to emulate for maize, but its comparatively large emulation error (compare open squares to lines in T case) is still smaller
than the spread simply due to different T patterns across climate simulations (Figure 11, left, compare differences between
open squares and line with the spread in circles for a given temperature value). Uncertainties in the yield damage function due
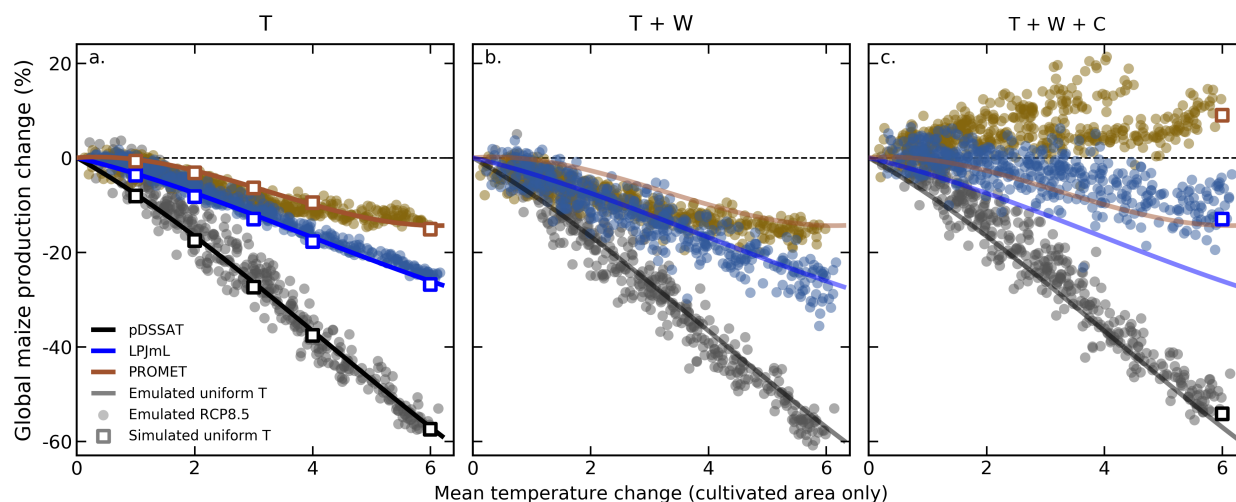
Figure 11. Illustration of the factors affecting yields in more realistic climate scenarios, for three different crop models. Figure shows emulated yield changes (relative to 1981-2010) for maize (both rainfed and irrigated) on currently cultivated land under RCP8.5 climate projections from 5 representative CMIP-5 climate models, using changes to T only (**a**), to T and W (**b**), and to T, W, and C (**c**). X-axis is the mean growing-season temperature change over cultivated land, computed using the historical growing season; note these values will be higher than the corresponding global mean temperature change. Circles are emulated yearly global production changes to 2100 (90 years × 5 climate timeseries = 450 per crop model), with x-axis the mean historical growing-season T shift over all grid cells where maize is grown (unweighted by within-cell cultivated area). **a:** Using only temperature changes allows comparing regional simulated and emulated values. Open squares are simulated values for each T level, with CWN at baseline; bold lines are emulated values over uniform T shifts (repeated in each panel). Emulation uncertainty (compare squares to lines) is small relative to differences across climate and crop models, and mean yield changes are similar whether T changes are applied as a uniform shift or in a more realistic spatial pattern (compare lines to circles). **b:** Adding in precipitation changes increases yield spread across climate projections and depresses yield slightly. **c:** CO_2 fertilization is small in pDSSAT, moderate in LPJmL, and very large in PROMET. The separation of groups of points in PROMET (gold) results because CMIP-5 climate sensitivities differ by nearly a factor of two; points at far right are under HadGEM2-ES. In RCP8.5, the 30-year-average CO_2 at end of century is 807 ppm (Riahi et al., 2011). For comparison, open squares in **c** show GGCMI-II simulated production changes at T+6, W=0, C=810 ppm. (Note that in these climate projections, mean CO_2 levels when T > 5.8 degrees is 912 ppm.) See Supplemental Figures S14–15 for analogous figures for other crops (spring wheat and soybeans).

to projected patterns of temperature change are in turn smaller than spread due to differing model relationships of W and T

430   changes (Figure 11, middle), and for PROMET are enormously outweighed by uncertainty in climate sensitivity (Figure 11, right). While emulator fidelity is important to ensure, it is important to recognize that these other uncertainties will dominate any impacts assessment exercise. Note that the pattern-related yield effects are actually relatively small for maize. (In Figure 11, left, compare lines, which show yield changes under uniform temperature shifts, to circles, which show changes under realistic warming scenarios). Pattern-related yield effects can be larger for other crops, and the uncertainties due to climate

435   projection differences correspondingly larger: see for example soybeans in Supplemental Figure S15.

6 Discussion and conclusions

In this work we describe a new class of global gridded crop model emulators for 5 crops (maize, soy, rice and spring and winter wheat) and 9 process-based crop models, based on the GGCMI Phase II dataset. The systematic parameter sampling of the GGCMI Phase II experiment allows emulating climatological-mean crop yield responses with a relatively simple statistical
440 model and isolating long-term impacts from confounding factors that lead to different year-to-year responses. Across all models, emulation errors over currently cultivated land never exceed 5% of yield changes at either global or regional scale. The systematic sampling provides information on the influence of multiple interacting factors in a way that realistic climate model simulations cannot, and the use of a parametric statistical model allows physical interpretation of parameter values. While emulators based on the GGCMI Phase II protocol of uniform perturbations to historical climate will not reproduce any effects
445 of changing variability in future climate projections (any temperature variability changes or precipitation variability changes other than multiplicative mean shifts), in practice these effects appear to be small, at least on the regionally aggregated level.

Emulators provide powerful tools for both model comparison and impacts assessments by capturing the responses of process-based crop models in a lightweight form. The emulators provide over three orders of magnitude reduction in data storage: the yield output for a single crop model that simulates all GGCMIP Phase II scenarios for 5 crops is $\sim$12.5 GB; equivalent global
450 gridded emulator parameters are only $\sim$20 MB and allow emulation of arbitrary future scenarios. Computational requirements are nearly negligible: a thousand years of global 0.5 degree yields, i.e $\sim$40,000,000 individual yield projections, can be emulated in 20 seconds on a laptop computer. The emulators can be used to develop standalone damage functions at any geographic scale larger that 0.5 degrees, or can be integrated directly into a larger integrated assessment model (IAM) framework.

Several cautions should be noted when using the emulators presented here. First, extrapolation outside the GGCMI Phase II
455 sample space should be avoided. Second, while the emulators are valuable for understanding the shape of yield responses and the factors that drive them, the absolute values of emulated yields should be treated with caution. Because the GGCMI Phase II experiment was designed to focus on yield changes and not on replicating real-world yields, most models are not formally calibrated, and their emulators should be used for absolute impacts projections only in combination with historical yield data.

The GGCMI Phase II dataset and emulators invite a broad range of potential future avenues of analysis. Future studies
460 using the emulators described here could include a detailed examination of interaction terms, robust quantification of model sensitivities to input drivers, and evaluation of geographic shifts in optimal growing regions. Studies of yield responses to changes in growing-season variability would require new simulations, but the emulators presented here provide a ready means of testing the null hypothesis that such effects are small. Similar structured training sets could be constructed to directly study responses to variability changes: see e.g. Poppick et al. (2016); Haugen et al. (2018) for methods of constructing synthetic
465 climate timeseries with altered variability. The GGCMI Phase II dataset can be used as a testbed for examining the ability of statistical models using more detailed within-season regressors to capture both year-over-year and climatological changes, and for more systematic studies of emulation itself, including evaluation of alternate specifications or machine learning methods. In general, the GGCMI Phase II experiment demonstrates the promise and utility of systematic parameter sweeps for improving understanding of the factors driving crop responses and for evaluating and improving process-based crop models.

470 *Code and data availability.* The polynomial parameters for crop model emulators are available at https://doi.org/10.5281/zenodo.3592453.

Author contributions. J.E., C.M, A.R., J.F., and E.M. designed the research. C.M., J.J., P.F., C.F., L.F., R.C.I., I.J., C.J., W.L., S.O., M.P., T.P., A.Re., K.W., and F.Z. performed the simulations. J.F., J.J., A.S., M.L., Z.W., and E.M. performed the analysis and J.F., C.M., and E.M. prepared the manuscript.

Competing interests. The authors declare no competing interests.

475 *Acknowledgements.* We thank Michael Stein and Kevin Schwarzwald, who provided helpful suggestions that contributed to this work. This research was performed as part of the Center for Robust Decision-making on Climate and Energy Policy (RDCEP) at the University of Chicago, and was supported through a variety of sources. RDCEP is funded by NSF grant #SES-1463644 through the Decision Making Under Uncertainty program. J.F. was supported by the NSF NRT program, grant #DGE-1735359 and by an NSF Graduate Research Fellowship, grant #DGE-1746045. C.M. was supported by the MACMIT project (01LN1317A) funded through the German Federal Ministry of Educa-
480 tion and Research (BMBF). C.F. was supported by the European Research Council Synergy grant #ERC-2013-SynG-610028 Imbalance-P. P.F. and K.W. were supported by the Newton Fund through the Met Office Climate Science for Service Partnership Brazil (CSSP Brazil). K.W. was supported by the IMPREX research project supported by the European Commission under the Horizon 2020 Framework programme, grant #641811. A.S. was supported by the Office of Science of the U.S. Department of Energy as part of the Multi-sector Dynamics Research Program Area. S.O. acknowledges support from the Swedish strong research areas BECC and MERGE together with support from
485 LUCCI (Lund University Centre for studies of Carbon Cycle and Climate Interactions). R.C.I. acknowledges support from the Texas Agrilife Research and Extension, Texas A & M University. This is paper number 36 of the Birmingham Institute of Forest Research. Computing resources were provided by the University of Chicago Research Computing Center (RCC).

This material is based upon work supported by the National Science Foundation Graduate Research Fellowship Program under Grant No. (DGE-1746045). Any opinions, findings, and conclusions or recommendations expressed in this material are those of the authors and do
490 not necessarily reflect the views of the National Science Foundation.

References

Aulakh, M. S. and Malhi, S. S.: Interactions of Nitrogen with Other Nutrients and Water: Effect on Crop Yield and Quality, Nutrient Use Efficiency, Carbon Sequestration, and Environmental Pollution, Advances in Agronomy, 86, 341 – 409, https://doi.org/10.1016/S0065-2113(05)86007-9, 2005.

495 Blanc, E.: Statistical emulators of maize, rice, soybean and wheat yields from global gridded crop models, Agricultural and Forest Meteorology, 236, 145 – 161, https://doi.org/10.1016/j.agrformet.2016.12.022, 2017.

Blanc, E. and Sultan, B.: Emulating maize yields from global gridded crop models using statistical estimates, Agricultural and Forest Meteorology, 214-215, 134 – 147, https://doi.org/10.1016/j.agrformet.2015.08.256, 2015.

Castruccio, S., McInerney, D. J., Stein, M. L., Liu Crouch, F., Jacob, R. L., and Moyer, E. J.: Statistical Emulation of Climate Model Projections Based on Precomputed GCM Runs, Journal of Climate, 27, 1829–1844, https://doi.org/10.1175/JCLI-D-13-00099.1, 2014.

Challinor, A., Wheeler, T., Craufurd, P., Slingo, J., and Grimes, D.: Design and optimisation of a large-area process-based model for annual crops, Agricultural and Forest Meteorology, 124, 99 – 120, https://doi.org/https://doi.org/10.1016/j.agrformet.2004.01.002, http://www.sciencedirect.com/science/article/pii/S0168192304000085, 2004.

Conti, S., Gosling, J. P., Oakley, J. E., and O'Hagan, A.: Gaussian process emulation of dynamic computer codes, Biometrika, 96, 663–676, https://doi.org/10.1093/biomet/asp028, 2009.

Dee, D. P., Uppala, S., Simmons, A., Berrisford, P., Poli, P., Kobayashi, S., Andrae, U., Balmaseda, M., Balsamo, G., Bauer, d. P., et al.: The ERA-Interim reanalysis: Configuration and performance of the data assimilation system, Quarterly Journal of the royal meteorological society, 137, 553–597, 2011.

Dury, M., Hambuckers, A., Warnant, P., Henrot, A., Favre, E., Ouberdous, M., and François, L.: Responses of European forest ecosystems to 21st century climate: assessing changes in interannual variability and fire intensity, iForest - Biogeosciences and Forestry, pp. 82–99, https://doi.org/10.3832/ifor0572-004, 2011.

Elliott, J., Kelly, D., Chryssanthacopoulos, J., Glotter, M., Jhunjhnuwala, K., Best, N., Wilde, M., and Foster, I.: The parallel system for integrating impact models and sectors (pSIMS), Environmental Modelling and Software, 62, 509–516, https://doi.org/10.1016/j.envsoft.2014.04.008, 2014.

515 Ferrise, R., Moriondo, M., and Bindi, M.: Probabilistic assessments of climate change impacts on durum wheat in the Mediterranean region, Natural Hazards and Earth System Sciences, 11, 1293–1302, https://doi.org/10.5194/nhess-11-1293-2011, 2011.

Folberth, C., Gaiser, T., Abbaspour, K. C., Schulin, R., and Yang, H.: Regionalization of a large-scale crop growth model for sub-Saharan Africa: Model setup, evaluation, and estimation of maize yields, Agriculture, Ecosystems & Environment, 151, 21 – 33, https://doi.org/10.1016/j.agee.2012.01.026, 2012.

520 Franke, J., Müller, C., Elliott, J., Ruane, A. C., Jagermeyr, J., Balkovic, J., Ciais, P., Dury, M., Falloon, P., Folberth, C., Francois, L., Hank, T., Hoffmann, M., Izaurralde, R. C., Jacquemin, I., Jones, C., Khabarov, N., Koch, M., Li, M., Liu, W., Olin, S., Phillips, M., Pugh, T. A. M., Reddy, A., Wang, X., Williams, K., Zabel, F., and Moyer, E.: The GGCMI Phase II experiment: global gridded crop model simulations under uniform changes in CO_2, temperature, water, and nitrogen levels (protocol version 1.0), Geoscientific Model Development Discussions, 2019, 1–30, https://doi.org/10.5194/gmd-2019-237, https://www.geosci-model-dev-discuss.net/gmd-2019-237/, 2019.

525 Frieler, K., Lange, S., Piontek, F., Reyer, C. P. O., Schewe, J., Warszawski, L., Zhao, F., Chini, L., Denvil, S., Emanuel, K., Geiger, T., Halladay, K., Hurtt, G., Mengel, M., Murakami, D., Ostberg, S., Popp, A., Riva, R., Stevanovic, M., Suzuki, T., Volkholz, J., Burke, E., Ciais, P., Ebi, K., Eddy, T. D., Elliott, J., Galbraith, E., Gosling, S. N., Hattermann, F., Hickler, T., Hinkel, J., Hof, C., Huber, V.,

Jägermeyr, J., Krysanova, V., Marcé, R., Müller Schmied, H., Mouratiadou, I., Pierson, D., Tittensor, D. P., Vautard, R., van Vliet, M., Biber, M. F., Betts, R. A., Bodirsky, B. L., Deryng, D., Frolking, S., Jones, C. D., Lotze, H. K., Lotze-Campen, H., Sahajpal, R., Thonicke, K., Tian, H., and Yamagata, Y.: Assessing the impacts of 1.5^{o}C global warming — Simulation protocol of the Inter-Sectoral Impact Model Intercomparison Project (ISIMIP2b), Geosci. Model Dev., 10, 4321–4345, https://doi.org/10.5194/gmd-10-4321-2017, 2017.

Fronzek, S., Pirttioja, N., Carter, T. R., Bindi, M., Hoffmann, H., Palosuo, T., Ruiz-Ramos, M., Tao, F., Trnka, M., Acutis, M., Asseng, S., Baranowski, P., Basso, B., Bodin, P., Buis, S., Cammarano, D., Deligios, P., Destain, M.-F., Dumont, B., Ewert, F., Ferrise, R., François, L., Gaiser, T., Hlavinka, P., Jacquemin, I., Kersebaum, K. C., Kollas, C., Krzyszczak, J., Lorite, I. J., Minet, J., Minguez, M. I., Montesino, M., Moriondo, M., Müller, C., Nendel, C., Öztürk, I., Perego, A., Rodríguez, A., Ruane, A. C., Ruget, F., Sanna, M., Semenov, M. A., Slawinski, C., Stratonovitch, P., Supit, I., Waha, K., Wang, E., Wu, L., Zhao, Z., and Rötter, R. P.: Classifying multi-model wheat yield impact response surfaces showing sensitivity to temperature and precipitation change, Agricultural Systems, 159, 209–224, https://doi.org/10.1016/j.agsy.2017.08.004, 2018.

Gadgil, S., Rao, P. S., and Rao, K. N.: Use of climate information for farm-level decision making: rainfed groundnut in southern India, Agricultural Systems, 74, 431 – 457, https://doi.org/10.1016/S0308-521X(02)00049-5, 2002.

Glotter, M., Elliott, J., McInerney, D., Best, N., Foster, I., and Moyer, E. J.: Evaluating the utility of dynamical downscaling in agricultural impacts projections, Proceedings of the National Academy of Sciences, 111, 8776–8781, https://doi.org/10.1073/pnas.1314787111, 2014.

Glotter, M., Moyer, E., Ruane, A., and Elliott, J.: Evaluating the Sensitivity of Agricultural Model Performance to Different Climate Inputs, Journal of Applied Meteorology and Climatology, 55, 151113145618 001, https://doi.org/10.1175/JAMC-D-15-0120.1, 2015.

Hank, T., Bach, H., and Mauser, W.: Using a Remote Sensing-Supported Hydro-Agroecological Model for Field-Scale Simulation of Heterogeneous Crop Growth and Yield: Application for Wheat in Central Europe, Remote Sensing, 7, 3934–3965, https://doi.org/10.3390/rs70403934, 2015.

Hansen, J. and Jones, J.: Scaling-up crop models for climate variability applications, Agricultural Systems, 65, 43 – 72, https://doi.org/10.1016/S0308-521X(00)00025-1, 2000.

Haugen, M., Stein, M., Moyer, E., and Sriver, R.: Estimating changes in temperature distributions in a large ensemble of climate simulations using quantile regression, Journal of Climate, 31, 8573–8588, https://doi.org/10.1175/JCLI-D-17-0782.1, 2018.

He, W., Yang, J., Zhou, W., Drury, C., Yang, X., D. Reynolds, W., Wang, H., He, P., and Li, Z.-T.: Sensitivity analysis of crop yields, soil water contents and nitrogen leaching to precipitation, management practices and soil hydraulic properties in semi-arid and humid regions of Canada using the DSSAT model, Nutrient Cycling in Agroecosystems, 106, 201–215, https://doi.org/10.1007/s10705-016-9800-3, 2016.

Holden, P., Edwards, N., PH, G., Fraedrich, K., Lunkeit, F., E, K., Labriet, M., Kanudia, A., and F, B.: PLASIM-ENTSem v1.0: A spatiotemporal emulator of future climate change for impacts assessment, Geoscientific Model Development, 7, 433–451, https://doi.org/10.5194/gmd-7-433-2014, 2014.

Holzkämper, A., Calanca, P., and Fuhrer, J.: Statistical crop models: Predicting the effects of temperature and precipitation changes, Climate Research, 51, 11–21, https://doi.org/10.3354/cr01057, 2012.

Howden, S. and Crimp, S.: Assessing dangerous climate change impacts on Australia's wheat industry, Modelling and Simulation Society of Australia and New Zealand, pp. 505–511, https://doi.org/-, 2005.

Ingestad, T.: Nitrogen and Plant Growth; Maximum Efficiency of Nitrogen Fertilizers, Ambio, 6, 146–151, 1977.

Izaurralde, R., Williams, J., Mcgill, W., Rosenberg, N., and Quiroga Jakas, M.: Simulating soil C dynamics with EPIC: Model description and testing against long-term data, Ecological Modelling, 192, 362–384, https://doi.org/10.1016/j.ecolmodel.2005.07.010, 2006.

Jones, C. D., Hughes, J. K., Bellouin, N., Hardiman, S. C., Jones, G. S., Knight, J., Liddicoat, S., O'Connor, F. M., Andres, R. J., Bell, C., Boo, K.-O., Bozzo, A., Butchart, N., Cadule, P., Corbin, K. D., Doutriaux-Boucher, M., Friedlingstein, P., Gornall, J., Gray, L., Halloran, P. R., Hurtt, G., Ingram, W. J., Lamarque, J.-F., Law, R. M., Meinshausen, M., Osprey, S., Palin, E. J., Parsons Chini, L., Raddatz, T., Sanderson, M. G., Sellar, A. A., Schurer, A., Valdes, P., Wood, N., Woodward, S., Yoshioka, M., and Zerroukat, M.: The HadGEM2-
570   ES implementation of CMIP5 centennial simulations, Geoscientific Model Development, 4, 543–570, https://doi.org/10.5194/gmd-4-543-2011, 2011.

Jones, J., Hoogenboom, G., Porter, C., Boote, K., Batchelor, W., Hunt, L., Wilkens, P., Singh, U., Gijsman, A., and Ritchie, J.: The DSSAT cropping system model, European Journal of Agronomy, 18, 235 – 265, https://doi.org/10.1016/S1161-0301(02)00107-7, 2003.

Li, Y., Guan, K., Schnitkey, G. D., DeLucia, E., and Peng, B.: Excessive rainfall leads to maize yield loss of a comparable magnitude to
575   extreme drought in the United States, Global Change Biology, 25, 2325–2337, https://doi.org/10.1111/gcb.14628, 2019.

Lindeskog, M., Arneth, A., Bondeau, A., Waha, K., Seaquist, J., Olin, S., and Smith, B.: Implications of accounting for land use in simulations of ecosystem carbon cycling in Africa, Earth System Dynamics, 4, 385–407, https://doi.org/10.5194/esd-4-385-2013, 2013.

Liu, B., Asseng, S., Müller, C., Ewert, F., Elliott, J., Lobell, D. B., Martre, P., Ruane, A. C., Wallach, D., Jones, J. W., et al.: Similar estimates of temperature impacts on global wheat yield by three independent methods, Nature Climate Change, 6, 1130, 2016a.

580   Liu, J., Williams, J. R., Zehnder, A. J., and Yang, H.: GEPIC - modelling wheat yield and crop water productivity with high resolution on a global scale, Agricultural Systems, 94, 478 – 493, https://doi.org/10.1016/j.agsy.2006.11.019, 2007.

Liu, W., Yang, H., Folberth, C., Wang, X., Luo, Q., and Schulin, R.: Global investigation of impacts of PET methods on simulating crop-water relations for maize, Agricultural and Forest Meteorology, 221, 164 – 175, https://doi.org/10.1016/j.agrformet.2016.02.017, 2016b.

Liu, W., Yang, H., Liu, J., Azevedo, L. B., Wang, X., Xu, Z., Abbaspour, K. C., and Schulin, R.: Global assessment of ni-
585   trogen losses and trade-offs with yields from major crop cultivations, Science of The Total Environment, 572, 526 – 537, https://doi.org/10.1016/j.scitotenv.2016.08.093, 2016c.

Lobell, D. B. and Burke, M. B.: On the use of statistical models to predict crop yield responses to climate change, Agricultural and Forest Meteorology, 150, 1443 – 1452, https://doi.org/10.1016/j.agrformet.2010.07.008, 2010.

Lobell, D. B. and Field, C. B.: Global scale climate-crop yield relationships and the impacts of recent warming, Environmental Research
590   Letters, 2, 014 002, https://doi.org/10.1088/1748-9326/2/1/014002, 2007.

MacKay, D.: Bayesian Interpolation, Neural Computation, 4, 415–447, https://doi.org/10.1162/neco.1992.4.3.415, 1991.

Makowski, D., Asseng, S., Ewert, F., Bassu, S., Durand, J., Martre, P., Adam, M., Aggarwal, P., Angulo, C., Baron, C., Basso, B., Bertuzzi, P., Biernath, C., Boogaard, H., Boote, K., Brisson, N., Cammarano, D., Challinor, A., Conijn, J., and Wolf, J.: Statistical Analysis of Large Simulated Yield Datasets for Studying Climate Effects, p. 1100, World Scientific Publishing Co,
595   https://doi.org/10.13140/RG.2.1.5173.8328, 2015.

Martin, T. H. D. T. G. M., Bellouin, N., Collins, W. J., Culverwell, I. D., Halloran, P. R., Hardiman, S. C., Hinton, T. J., Jones, C. D., McDonald, R. E., McLaren, A. J., O'Connor, F. M., Roberts, M. J., Rodriguez, J. M., Woodward, S., Best, M. J., Brooks, M. E., Brown, A. R., Butchart, N., Dearden, C., Derbyshire, S. H., Dharssi, I., Doutriaux-Boucher, M., Edwards, J. M., Falloon, P. D., Gedney, N., Gray, L. J., Hewitt, H. T., Hobson, M., Huddleston, M. R., Hughes, J., Ineson, S., Ingram, W. J., James, P. M., Johns, T. C., Johnson, C. E.,
600   Jones, A., Jones, C. P., Joshi, M. M., Keen, A. B., Liddicoat, S., Lock, A. P., Maidens, A. V., Manners, J. C., Milton, S. F., Rae, J. G. L., Ridley, J. K., Sellar, A., Senior, C. A., Totterdell, I. J., Verhoef, A., Vidale, P. L., and Wiltshire, A.: The HadGEM2 family of Met Office Unified Model climate configurations, Geoscientific Model Development, 4, 723–757, https://doi.org/10.5194/gmd-4-723-2011, 2011.

Mauser, W., Klepper, G., Zabel, F., Delzeit, R., Hank, T., Putzenlechner, B., and Calzadilla, A.: Global biomass production potentials exceed expected future demand without the need for cropland expansion, Nature Communications, 6, https://doi.org/10.1038/ncomms9946, 2015.

605 Minoli, S., Müller, C., Elliott, J., Ruane, A. C., Jägermeyr, J., Zabel, F., Dury, M., Folberth, C., François, L., Hank, T., Jacquemin, I., Liu, W., Olin, S., and Pugh, T. A.: Global response patterns of major rainfed crops to adaptation by maintaining current growing periods and irrigation, Earth's Future, 0, https://doi.org/10.1029/2018EF001130, https://agupubs.onlinelibrary.wiley.com/doi/abs/10.1029/2018EF001130, 2019.

Mistry, M. N., Wing, I. S., and De Cian, E.: Simulated vs. empirical weather responsiveness of crop yields: US evidence and implications
610 for the agricultural impacts of climate change, Environmental Research Letters, 12, https://doi.org/10.1088/1748-9326/aa788c, 2017.

Moore, F. C., Baldos, U., Hertel, T., and Diaz, D.: New science of climate change impacts on agriculture implies higher social cost of carbon, Nature Communications, 8, https://doi.org/10.1038/s41467-017-01792-x, 2017.

Nakamura, T., Osaki, M., Koike, T., Hanba, Y. T., Wada, E., and Tadano, T.: Effect of CO2 enrichment on carbon and nitrogen interaction in wheat and soybean, Soil Science and Plant Nutrition, 43, 789–798, https://doi.org/10.1080/00380768.1997.10414645, 1997.

615 O'Hagan, A.: Bayesian analysis of computer code outputs: A tutorial, Reliability Engineering & System Safety, 91, 1290 – 1300, https://doi.org/10.1016/j.ress.2005.11.025, 2006.

Olin, S., Schurgers, G., Lindeskog, M., Wårlind, D., Smith, B., Bodin, P., Holmér, J., and Arneth, A.: Modelling the response of yields and tissue C:N to changes in atmospheric CO_2 and N management in the main wheat regions of western Europe, Biogeosciences, 12, 2489–2515, https://doi.org/10.5194/bg-12-2489-2015, 2015.

620 Osaki, M., Shinano, T., and Tadano, T.: Carbon-nitrogen interaction in field crop production, Soil Science and Plant Nutrition, 38, 553–564, https://doi.org/10.1007/BF00025019, 1992.

Osborne, T., Gornall, J., Hooker, J., Williams, K., Wiltshire, A., Betts, R., and Wheeler, T.: JULES-crop: a parametrisation of crops in the Joint UK Land Environment Simulator, Geoscientific Model Development, 8, 1139–1155, https://doi.org/10.5194/gmd-8-1139-2015, 2015.

625 Ostberg, S., Schewe, J., Childers, K., and Frieler, K.: Changes in crop yields and their variability at different levels of global warming, Earth System Dynamics, 9, 479–496, https://doi.org/10.5194/esd-9-479-2018, 2018.

Oyebamiji, O. K., Edwards, N. R., Holden, P. B., Garthwaite, P. H., Schaphoff, S., and Gerten, D.: Emulating global climate change impacts on crop yields, Statistical Modelling, 15, 499–525, https://doi.org/10.1177/1471082X14568248, 2015.

Pedregosa, F., Varoquaux, G., Gramfort, A., Michel, V., Thirion, B., Grisel, O., Blondel, M., Prettenhofer, P., Weiss, R., Dubourg, V.,
630 Vanderplas, J., Passos, A., Cournapeau, D., Brucher, M., Perrot, M., and Duchesnay, E.: Scikit-learn: Machine Learning in Python, Journal of Machine Learning Research, 12, 2825–2830, 2011.

Pirttioja, N., Carter, T., Fronzek, S., Bindi, M., Hoffmann, H., Palosuo, T., Ruiz-Ramos, M., Tao, F., Trnka, M., Acutis, M., Asseng, S., Baranowski, P., Basso, B., Bodin, P., Buis, S., Cammarano, D., Deligios, P., Destain, M., Dumont, B., Ewert, F., Ferrise, R., François, L., Gaiser, T., Hlavinka, P., Jacquemin, I., Kersebaum, K., Kollas, C., Krzyszczak, J., Lorite, I., Minet, J., Minguez, M., Montesino, M., Moriondo, M.,
635 Müller, C., Nendel, C., Öztürk, I., Perego, A., Rodríguez, A., Ruane, A., Ruget, F., Sanna, M., Semenov, M., Slawinski, C., Stratonovitch, P., Supit, I., Waha, K., Wang, E., Wu, L., Zhao, Z., and Rötter, R.: Temperature and precipitation effects on wheat yield across a European transect: a crop model ensemble analysis using impact response surfaces, Climate Research, 65, 87–105, https://doi.org/10.3354/cr01322, 2015.

Poppick, A., McInerney, D. J., Moyer, E. J., and Stein, M. L.: Temperatures in transient climates: Improved methods for simulations with
640 evolving temporal covariances, Ann. Appl. Stat., 10, 477–505, https://doi.org/10.1214/16-AOAS903, 2016.

Portmann, F., Siebert, S., and Doell, P.: MIRCA2000 - Global Monthly Irrigated and Rainfed Crop Areas around the Year 2000: A New High-Resolution Data Set for Agricultural and Hydrological Modeling, Global Biogeochemical Cycles, 24, GB1011, https://doi.org/10.1029/2008GB003435, 2010.

Potter, N. J., Zhang, L., Milly, P. C. D., McMahon, T. A., and Jakeman, A. J.: Effects of rainfall seasonality and soil moisture capacity on mean annual water balance for Australian catchments, Water Resources Research, 41, https://doi.org/10.1029/2004WR003697, https://agupubs.onlinelibrary.wiley.com/doi/abs/10.1029/2004WR003697, 2005.

Räisänen, J. and Ruokolainen, L.: Probabilistic forecasts of near-term climate change based on a resampling ensemble technique, Tellus A: Dynamic Meteorology and Oceanography, 58, 461–472, https://doi.org/10.1111/j.1600-0870.2006.00189.x, 2006.

Ratto, M., Castelletti, A., and Pagano, A.: Emulation techniques for the reduction and sensitivity analysis of complex environmental models, Environmental Modelling & Software, 34, 1 – 4, https://doi.org/10.1016/j.envsoft.2011.11.003, 2012.

Razavi, S., Tolson, B. A., and Burn, D. H.: Review of surrogate modeling in water resources, Water Resources Research, 48, https://doi.org/10.1029/2011WR011527, 2012.

Riahi, K., Rao, S., Krey, V., Cho, C., Chirkov, V., Fischer, G., Kindermann, G., Nakicenovic, N., and Rafaj, P.: RCP 8.5—A scenario of comparatively high greenhouse gas emissions, Climatic Change, 109, 33, https://doi.org/10.1007/s10584-011-0149-y, 2011.

Roberts, M., Braun, N., R Sinclair, T., B Lobell, D., and Schlenker, W.: Comparing and combining process-based crop models and statistical models with some implications for climate change, Environmental Research Letters, 12, https://doi.org/10.1088/1748-9326/aa7f33., 2017.

Rosenzweig, C., Jones, J., Hatfield, J., Ruane, A., Boote, K., Thorburn, P., Antle, J., Nelson, G., Porter, C., Janssen, S., Asseng, S., Basso, B., Ewert, F., Wallach, D., Baigorria, G., and Winter, J.: The Agricultural Model Intercomparison and Improvement Project (AgMIP): Protocols and pilot studies, Agricultural and Forest Meteorology, 170, 166 – 182, https://doi.org/10.1016/j.agrformet.2012.09.011, 2013.

Rosenzweig, C., Elliott, J., Deryng, D., Ruane, A. C., Müller, C., Arneth, A., Boote, K. J., Folberth, C., Glotter, M., Khabarov, N., Neumann, K., Piontek, F., Pugh, T. A. M., Schmid, E., Stehfest, E., Yang, H., and Jones, J. W.: Assessing agricultural risks of climate change in the 21st century in a global gridded crop model intercomparison, Proceedings of the National Academy of Sciences, 111, 3268–3273, https://doi.org/10.1073/pnas.1222463110, 2014.

Ruane, A., I. Hudson, N., Asseng, S., Camarrano, D., Ewert, F., Martre, P., J. Boote, K., Thorburn, P., Aggarwal, P., Angulo, C., Basso, B., Bertuzzi, P., Biernath, C., Brisson, N., Challinor, A., Doltra, J., Gayler, S., Goldberg, R., Grant, R., and Wolf, J.: Multi-wheat-model ensemble responses to interannual climate variability, Environmental Modelling and Software, 81, 86–101, https://doi.org/10.1016/j.envsoft.2016.03.008, 2016.

Ruane, A. C., Cecil, L. D., Horton, R. M., Gordon, R., McCollum, R., Brown, D., Killough, B., Goldberg, R., Greeley, A. P., and Rosenzweig, C.: Climate change impact uncertainties for maize in Panama: Farm information, climate projections, and yield sensitivities, Agricultural and Forest Meteorology, 170, 132 – 145, https://doi.org/10.1016/j.agrformet.2011.10.015, 2013.

Ruane, A. C., McDermid, S., Rosenzweig, C., Baigorria, G. A., Jones, J. W., Romero, C. C., and Cecil, L. D.: Carbon-temperature-water change analysis for peanut production under climate change: A prototype for the AgMIP Coordinated Climate-Crop Modeling Project (C3MP), Glob. Change Biology, 20, 394–407, https://doi.org/10.1111/gcb.12412, 2014.

Ruane, A. C., Goldberg, R., and Chryssanthacopoulos, J.: Climate forcing datasets for agricultural modeling: Merged products for gap-filling and historical climate series estimation, Agric. Forest Meteorol., 200, 233–248, https://doi.org/10.1016/j.agrformet.2014.09.016, 2015.

Ruiz-Ramos, M., Ferrise, R., Rodríguez, A., Lorite, I., Bindi, M., Carter, T., Fronzek, S., Palosuo, T., Pirttioja, N., Baranowski, P., Buis, S., Cammarano, D., Chen, Y., Dumont, B., Ewert, F., Gaiser, T., Hlavinka, P., Hoffmann, H., Höhn, J., Jurecka, F., Kersebaum, K., Krzyszczak, J., Lana, M., Mechiche-Alami, A., Minet, J., Montesino, M., Nendel, C., Porter, J., Ruget, F., Semenov, M., Steinmetz, Z., Stratonovitch,

P., Supit, I., Tao, F., Trnka, M., de Wit, A., and Rötter, R.: Adaptation response surfaces for managing wheat under perturbed climate and
CO2 in a Mediterranean environment, Agricultural Systems, 159, 260 – 274, https://doi.org/10.1016/j.agsy.2017.01.009, 2018.

Schlenker, W. and Roberts, M. J.: Nonlinear temperature effects indicate severe damages to U.S. crop yields under climate change, Proceedings of the National Academy of Sciences, 106, 15 594–15 598, https://doi.org/10.1073/pnas.0906865106, 2009.

Snyder, A., Calvin, K. V., Phillips, M., and Ruane, A. C.: A crop yield change emulator for use in GCAM and similar models:Persephone
v1.0, Geoscientific Model Development, 12, 1319–1350, https://doi.org/10.5194/gmd-12-1319-2019, https://www.geosci-model-dev.net/
12/1319/2019/, 2019.

Storlie, C. B., Swiler, L. P., Helton, J. C., and Sallaberry, C. J.: Implementation and evaluation of nonparametric regression procedures for sensitivity analysis of computationally demanding models, Reliability Engineering & System Safety, 94, 1735 – 1763,
https://doi.org/10.1016/j.ress.2009.05.007, 2009.

Taylor, K. E., Stouffer, R. J., and Meehl, G. A.: An Overview of CMIP5 and the Experiment Design, Bulletin of the American Meteorological
Society, 93, 485–498, https://doi.org/10.1175/BAMS-D-11-00094.1, 2012.

Tebaldi, C. and Lobell, D. B.: Towards probabilistic projections of climate change impacts on global crop yields, Geophysical Research
Letters, 35, https://doi.org/10.1029/2008GL033423, 2008.

Urban, D., Roberts, M. J., Schlenker, W., and Lobell, D. B.: Projected temperature changes indicate significant increase in interannual
variability of U.S. maize yields: A Letter, Climatic Change, 112, 525–533, https://doi.org/10.1007/s10584-012-0428-2, 2012.

von Bloh, W., Schaphoff, S., Müller, C., Rolinski, S., Waha, K., and Zaehle, S.: Implementing the Nitrogen cycle into the dynamic global vegetation, hydrology and crop growth model LPJmL (version 5.0), Geoscientific Model Development, 11, 2789–2812,
https://doi.org/10.5194/gmd-11-2789-2018, 2018.

Warszawski, L., Frieler, K., Huber, V., Piontek, F., Serdeczny, O., and Schewe, J.: The Inter-Sectoral Impact Model Intercomparison Project (ISI–MIP): Project framework, Proceedings of the National Academy of Sciences, 111, 3228–3232,
https://doi.org/10.1073/pnas.1312330110, 2014.

Weedon, G. P., Balsamo, G., Bellouin, N., Gomes, S., Best, M. J., and Viterbo, P.: The WFDEI meteorological forcing data set: WATCH
Forcing Data methodology applied to ERA-Interim reanalysis data, Water Resources Research, 50, 7505–7514, 2014.

Williams, K., Gornall, J., Harper, A., Wiltshire, A., Hemming, D., Quaife, T., Arkebauer, T., and Scoby, D.: Evaluation of JULES-crop
performance against site observations of irrigated maize from Mead, Nebraska, Geoscientific Model Development, 10, 1291–1320,
https://doi.org/10.5194/gmd-10-1291-2017, 2017.

Williams, K. E. and Fallon, P. D.: Sources of interannual yield variability in JULES-crop and implications for forcing with seasonal weather
forecasts, Geoscientific Model Development, 8, 3987–3997, https://doi.org/10.5194/gmd-8-3987-2015, 2015.

Zabel, F., Delzeit, R., Schneider, J. M., Seppelt, R., Mauser, W., and Vàclavík, T.: Global impacts of future cropland expansion and intensification on agricultural markets and biodiversity, Nature Communications, 10, 2844, https://doi.org/10.1038/s41467-019-10775-z,
http://www.nature.com/articles/s41467-019-10775-z, 2019.

Zhao, C., Liu, B., Piao, S., Wang, X., Lobell, D. B., Huang, Y., Huang, M., Yao, Y., Bassu, S., Ciais, P., Durand, J. L., Elliott, J., Ewert, F.,
Janssens, I. A., Li, T., Lin, E., Liu, Q., Martre, P., Müller, C., Peng, S., Peñuelas, J., Ruane, A. C., Wallach, D., Wang, T., Wu, D., Liu,
Z., Zhu, Y., Zhu, Z., and Asseng, S.: Temperature increase reduces global yields of major crops in four independent estimates, Proc. Natl.
Acad. Sci., 114, 9326–9331, https://doi.org/10.1073/pnas.1701762114, 2017.